Bioactive Materials 42 (2024) 587–612

Contents lists available at ScienceDirect

Bioactive Materials

journal homepage: www.keaipublishing.com/en/journals/bioactive-materials

Review article

Biliary stents for active materials and surface modification: Recent advances and future perspectives

Yuechuan Li [a,c,1], Kunshan Yuan [a,c,1], Chengchen Deng [a,c,1], Hui Tang [b,c], Jinxuan Wang [d], Xiaozhen Dai [d], Bing Zhang [e], Ziru Sun [c,f], Guiying Ren [c,f], Haijun Zhang [b,c,**], Guixue Wang [a,d,e,*]

[a] Key Laboratory for Biorheological Science and Technology of Ministry of Education, National Local Joint Engineering Laboratory for Vascular Implants, Bioengineering College of Chongqing University, Chongqing, 400044, China
[b] Shanghai Tenth People's Hospital, School of Medicine, Tongji University, Shanghai, 200092, China
[c] National United Engineering Laboratory for Biomedical Material Modification, Dezhou, 251100, China
[d] School of Biosciences and Technology, Chengdu Medical College, Chengdu, 610500, China
[e] Nanjing Key Laboratory for Cardiovascular Information and Health Engineering Medicine (CVIHEM), Drum Tower Hospital, Nanjing University, Nanjing, China
[f] College of materials science and engineering, Shandong University of Technology, Zibo, 25500, Shandong, China

ARTICLE INFO

Keywords:
Biliary stent
Biodegradable
Functional coatings
Tissue engineering & 3D-printed stent
Shape memory

ABSTRACT

Demand for biliary stents has expanded with the increasing incidence of biliary disease. The implantation of plastic or self-expandable metal stents can be an effective treatment for biliary strictures. However, these stents are nondegradable and prone to restenosis. Surgical removal or replacement of the nondegradable stents is necessary in cases of disease resolution or restenosis. To overcome these shortcomings, improvements were made to the materials and surfaces used for the stents. First, this paper reviews the advantages and limitations of nondegradable stents. Second, emphasis is placed on biodegradable polymer and biodegradable metal stents, along with functional coatings. This also encompasses tissue engineering & 3D-printed stents were highlighted. Finally, the future perspectives of biliary stents, including pro-epithelialization coatings, multifunctional coated stents, biodegradable shape memory stents, and 4D bioprinting, were discussed.

1. Introduction

The biliary system consists of the bile ducts and gallbladder, whose special structure and function contribute to the storage, transport, and excretion of bile, and the maintenance of the normal digestive process. Nevertheless, the global incidence of bile duct and gallbladder diseases rose dramatically from 26.35 million in 1990 to 52 million in 2019 [1]. Biliary strictures were observed in a considerable percentage of these patients, posing a serious threat to life and health [2].

Biliary strictures are classified as benign and malignant strictures. The possible etiologies of biliary strictures are shown in Fig. 1, [2]. Benign biliary strictures are mainly caused by postoperative damage (e.g., cholecystectomy, liver transplantation), inflammatory diseases, and gallstones. Whereas cholangiocarcinoma and pancreatic cancer are the principal reasons for malignant biliary strictures. The narrowed bile ducts prevent the flow of bile from the liver and gallbladder to the duodenum, leading to digestive abnormalities, cirrhosis, and jaundice [3].

Surgical intervention or stent implantation by percutaneous transhepatic biliary drainage or endoscopic retrograde cholangiopancreatography (ERCP) are the routine ways to restore biliary patency. ERCP is favored for its safety and low complications [4]. In addition, stents can be applied to bile leaks, fistulae, as well as other biliary diseases [5]. According to Global Market Insight, the size of the biliary stent market exceeded USD 394.5 million in 2022 and is predicted to register a CAGR of more than 5.5 % during 2023–2032. However, the most commonly plastic or self-expandable metal stents are

Peer review under responsibility of KeAi Communications Co., Ltd.
* Corresponding author. Key Laboratory for Biorheological Science and Technology of Ministry of Education, National Local Joint Engineering Laboratory for Vascular Implants, Bioengineering College of Chongqing University, Chongqing, 400044, China.
** Corresponding author. Shanghai Tenth People's Hospital, School of Medicine, Tongji University, Shanghai, 200092, China.
E-mail addresses: zhanghaijun@tongji.edu.cn (H. Zhang), wanggx@cqu.edu.cn (G. Wang).
[1] Co-first authors.

https://doi.org/10.1016/j.bioactmat.2024.08.031
Received 3 May 2024; Received in revised form 27 August 2024; Accepted 27 August 2024

nondegradable and need to be promptly removed or replaced, when the benign strictures have been resolved or in-stent restenosis are encountered. These additional operations may be accompanied by risks that increase the burden on patients.

The disadvantages of traditional stents, such as non-degradability and susceptibility to restenosis [6], have led to the development of a new generation of biliary stents. Improvements for biliary stents mainly include materials and surface modifications. Biodegradable stents have attracted increasing.

attention due to their biodegradability, no additional intervention required, and absence of severe complications [7]. Moreover, surface modification technologies (antitumor coatings, stone-dissolving coatings, antibacterial or antibiofilm coatings, antiproliferative coatings, and corrosion-resistant coatings) have also been introduced to prolong stent patency and reduce complications. Furthermore, tissue engineering and 3D printing technologies could address the lack of personalization of stents made by traditional preparation methods, which are intended for rapid bile duct reconstruction or repair [4].

This review outlined the advantages and limitations of nondegradable biliary stents. Second, the biodegradable biliary stents, functional coatings, tissue engineering and 3D-printed stents were highlighted. Finally, possible future directions were discussed, including pro-epithelialization coatings, multifunctional coated stents, biodegradable shape memory stents, and 4D bioprinting.

2. Nondegradable biliary stents

Plastic stent (PS) and self-expandable metal stent (SEMS) are the main types of nondegradable biliary stents. SEMS can be further classified into uncovered SEMS and covered SEMS on the basis of the presence or absence of a covering. Typical biliary stents are shown in Fig. 2.

2.1. Plastic biliary stents

PS was the first stent used to treat biliary benign strictures and bile leak [4]. Polyethylene (PE), polyurethane (PU), Teflon, polytetrafluoroethylene (PTFE), PE/PU blend, or soft polymer blend is common materials used to fabricate PS [8]. PS is available in a variety of shapes, including straight.

curved, pigtails (single or double pigtails), etc. PS is generally incorporated with side holes as well as flanges or pigtails for better drainage and to prevent migration, respectively. Since the PS is radiopaque, both ends of the stent are usually labeled with radiomarkers to facilitate proper implantation of the stent in the bile duct and subsequent examination [9]. Due to its effectiveness, low cost, ease of insertion, and removal, PS is widely used [10–12]. Nevertheless, it is still confronted with the following drawbacks: 1) Stent occlusion: bacterial biofilm formation was the main culprit [6]. Therefore, the PS will be replaced or removed every 3–4 months to reduce the risk of clogging [2,13,14]. 2) Stent migration: the overall migration rate of PS in patients with benign and malignant conditions was 8.58 % [15].

Although substantial improvements have been made to PS, the short patency needs to be defeated. The development of more flexible preparation materials to reduce stent migration and facilitate delivery is possible. Alternatively, materials with antibacterial properties, high-efficiency anti-reflux, anti-migration systems, and advanced surface modification technologies (see below) can also be brought into PS to extend the patency.

2.2. Self-expandable metal stents

Stents with larger diameter usually have longer patency [16,17]. This is explained by the larger diameter, the faster the bile flow rate and the lower the tendency for protein aggregation, bile salt deposition, and biofilm formation [18]. Due to the diameter of the working channel of most standard duodenoscopes is 4.2 mm [9], which prevents the introduction of PS with larger diameter. As a result, SEMS was invented to address the short patency of PS. SEMS is constrained by an external sheath during insertion through the duodenoscope channel. After retraction of the sheath, the stent is expanded at the target, with a diameter of 6–10 mm. Some SEMSs have a retrieval loop to make it easier to reposition or retrieve the stent after it has been placed. Platinol, stainless steel, and nitinol are used in preparing SEMS [4]. Nitinol stents have become mainstream due to their shape memory and super-elastic properties. SEMS is mainly produced by laser cutting or braiding, and its mesh structure can be divided into closed-cell type and open-cell type. Closed-cell stents with less flexibility and may incomplete complexity or expansion. The open-cell stents are more appropriate for curved or complex anatomical structures [19]. Depending on the braiding techniques, stents are classified as cross type, hook type, and cross & hook type, as shown in Fig. 2I–K. Most manufacturers have adopted the cross & hook type to utilize the advantages of both structures [20]. Tumor ingrowth (tumor grows between stent mesh lines) or

Malignant, primary
●Pancreatic cancer, cholangiocarcinoma, gallbladder cancer, hepatocellular carcinoma, ampullary cancer, lymphoma
●Rare: cystadenocarcinomas, mixed hepatocellular-cholangiocellular cancer
Malignant, metastatic
●Breast cancer, colon cancer, renal cell cancer
●Rare: squamous cell carcinoma
Fibroinflammatory
●Chronic pancreatitis, primary sclerosing cholangitis, autoimmune (immunoglobulin G [IgG] 4-mediated) pancreatitis, IgG4-mediated cholangitis, sarcoidosis, recurrent pyogenic cholangitis, extrinsic compression by a pancreatic fluid collection
Iatrogenic
●Cholecystectomy, liver transplantation, local cancer treatment (chemoembolization, radiation therapy, microwave ablation, radiofrequency ablation)
Vascular
●Portal hypertensive biliopathy, ischemic biliary injury
AIDS cholangiopathy
Mirizzi syndrome

Fig. 1. Etiology of biliary strictures [2].

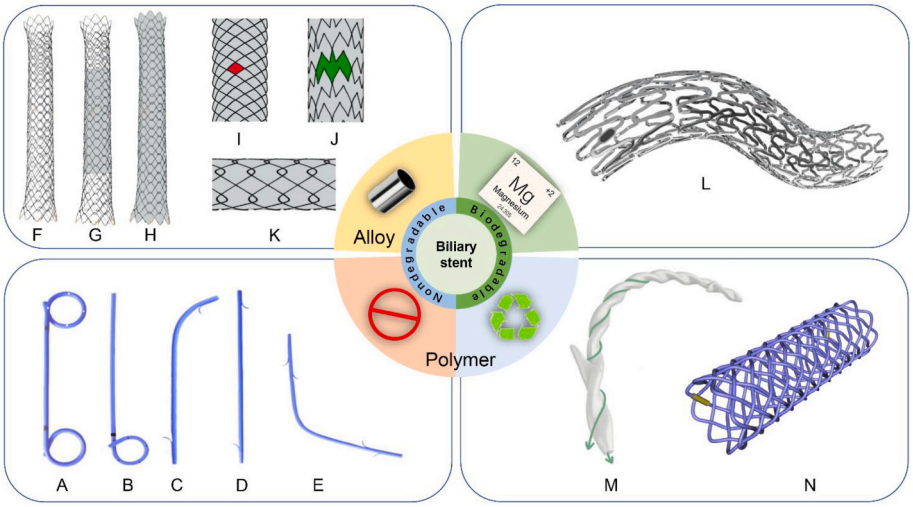

Fig. 2. Typical types of biliary stents. **A-E:** Nondegradable plastic stents. **A:** Double pigtails. **B:** Single pigtail. **C:** Curved. **D:** Straight. **E:** Amsterdam. **F-K:** Nondegradable metal stents. **F:** Uncovered self-expandable metal stent. **G:** Partially covered. **H:** Fully covered. **I:** Cross type, closed-cell (red mark), braided. **J:** Open cell (green mark), laser-cut. **K:** Cross & hook, braided. **L:** Biliary stent made of magnesium alloy (UNITY-B; AMG International, Winsen, Germany). **M-N:** Biodegradable polymer stents. **M:** Archimedes stent (Amg International GmbH, Winsen, Germany). **N:** Ella-DV biliary stent made of polydioxanone (Ella-CS, Hradec Králové, Czech Republic).

overgrowth (the proximal or distal end of the stent is blocked by the tumor), tissue ingrowth, mucosal hyperplasia, or biliary sludge are the main causes of uncovered SEMS obstruction [6]. Tumor or tissue embedded in the stent also made it difficult to remove or reposition the stent. Covered SEMS is designed to mitigate these defects in uncovered SEMS.

Depending on the extent of the coverage, covered SEMS is further categorized into fully covered SEMS and partially covered SEMS. Commonly covering materials such as PTFE and silicone enable easy stent removal by preventing tumor or tissue growth through the mesh [6]. However, a high risk of stent migration (15–62.7 %) was observed in fully covered SEMS [21]. Partially covered SEMS is designed to decrease migration based on the principle that the naked end of the stent is firmly anchored to the bile duct [22]. However, the effectiveness of covered stents compared to bare stents remains controversial [23–25]. Additionally, polymeric membranes may act as a matrix for bile sludge, resulting in a higher occlusion rate [26]. The coverings may also block the opening of the cystic or pancreatic ducts, increasing the incidence of pancreatitis and cholecystitis [27]. Overall, SEMS (41.0 ± 9.8 weeks) has longer median patency than PS (14.4 ± 0.9 weeks) [28], but suffer from the following weaknesses: 1) Stent occlusion, which is mainly caused by tumor and tissue growth, mucosal hyperplasia, and biliary sludge; 2) High migration rate (mostly in covered SEMS).

To address the migration of covered stents, novel stent designs, including anchored flaps [29] equipped with fins or flared ends [30,31], and additional anchored PS [32] have been proven to significantly reduce stent migration, Fig. 3. To alleviate the tumor ingrowth in uncovered SEMS while reducing the migration of fully covered SEMS, Kulpatcharapong et al. [33] prepared multiple drainage holes in the covering. The newly designed stent had longer patency, less tumor ingrowth than the uncovered SEMS and reduced migration compared to the fully covered SEMS. The designs described above provided new insights into the reduction of stent defects. In the future, more effective, bile duct-adapted antimigration systems, as well as better-performing covering materials are desirable to be explored. Stent stenosis due to tumor growth, tissue hyperplasia, bacterial infection, etc., can also be reduced by using appropriate surface modification techniques and anti-reflux systems.

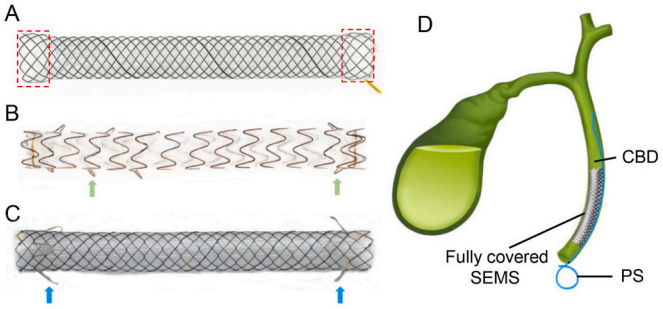

Fig. 3. Schematic for preventing stent migration. **A:** Fully covered SEMS with flared ends (red dashed boxes) [30]. **B:** Outward projecting wires as anchoring fins (green arrows) [30]. **C:** Fully covered SEMS with anchoring flaps at the proximal end of the stent (blue arrows) [29]. D: An externally anchored PS for extending the patency of fully covered SEMS [32]. SEMS: self-expandable metal stent. PS: plastic stent. CBD: common bile duct.

3. Novel biodegradable biliary stents

Non-degradability is the major drawback of PS and SEMS. Prompt removal or replacement of the stent was required when the stenosis had resolved or when in-stent restenosis occurred due to.

biofilm formation, tumor growth, and tissue hyperplasia. Optimally biliary stents should be fully degraded after completing its mission. Biodegradable materials are considered ideal for the manufacture of biliary stents because they degrades spontaneously, avoiding additional intervention. Typical polymers are polylactide (PLA), poly (L-lactic acid) (PLLA), poly (lactic-co-glycolic acid) (PLGA), polydioxanone (PDX), polycaprolactone (PCL), poly (vinyl alcohol) (PVA), and polyglycolide (PGA), Fig. 2.

3.1. PLA-based stents

PLA is an important material for stents and coatings fabrication due to its biocompatibility, degradability, and mechanical strength [34]. Barium sulfate is usually mixed in for making the stent radiopaque to allow observation. Several studies have shown that PLA biliary stents were biocompatible and degraded spontaneously within a few months,

as shown in Table 1. However, the presence of a mild inflammation response in the biliary mucosa, submucotic fibrosis, and vascularization requires attention. At a detailed molecular level, however, information on the bile duct response to PLA stent is still rather lacking. Siiki et al. [35] analyzed the change in protein levels of PLA stent acting in gastrointestinal stenosis after implantation in the bile duct. They found that the expression levels of galectin-2 and transgelin in the PLA stent group was restored to levels close to those in the native bile duct, which was different from the covered SEMS group. Whether these changes in protein levels are beneficial and the optimal protein expression associated with stenosis healing remain to be elucidated.

Due to its biocompatibility and biodegradability, PLLA has been employed in various implant, such as vascular stents [36]. Therefore, it may also be suitable for biliary stents. Two preliminary studies have shown the acceptable performance of PLLA stents in the bile duct [37, 38]. However, there is a discrepancy as to whether the PLLA stents were embedded in the bile duct or bile sludge was present, which may be related to the length of the study observation as well as the diameter and shape of the stent. Nevertheless, the acidic by-product of PLLA degradation may contribute to a local pH reduction causing an inflammatory response [36]. Furthermore, the inferior mechanical properties of PLLA, and the end of the PLLA molecular chain contains a free COOH group. The COO^- may absorb Ca^{2+} and thus facilitate the attachment of palmitate and unconjugated bilirubin [37]. These concerns about PLLA warrant validation with further research.

PLGA is a copolymer consisting of PLA and PGA, which can be tailored by adjusting the ratio of PLA/PGA for a variety of properties and characteristics, such as mechanical properties, degradation rate, and wettability [39]. These tunable properties and good biocompatibility allow PLGA to be used in nanomedicine, stent, and coating [40–42]. Several studies have explored its suitability as the biliary stents. Xu et al. [43] implanted PLGA (LA/GA = 71:29) stents into rats and found that stents deformation started after 3 weeks, and completely degraded within 4–5 weeks. Subsequently, they verified that PLGA (LA/GA = 80:20) stents were safe in canine bile duct and disappeared within 4–5 weeks [44]. These studies tentatively suggested that PLGA stent can provide short-term support for the bile duct. Importantly, the degradation rate of the stent can also be optimized by adjusting the ratio of LA/GA to prolong the duration of PLGA stent support.

Table 1
In vivo evaluation of biodegradable polymer stents.

Stent type	Diameter	Indication	Number	Main result	Ref
PLA	10 mm	CBD	8 Pigs	Biliary patency was good at 6 months postoperatively, with no biliary integration or proliferation.	[75]
PLA	6–7 mm	Cystic duct leakage	6 Pigs	The stents effectively managed bile leak and disappeared after 6 months.	[76]
PLA	6–9 mm	Hepaticojejunal anastomosis	25 Pigs	At 18-month follow-up, stent was biocompatible, degraded safely and may be linked to a larger and better drainage anastomosis.	[77]
PLA	4 mm	Hepaticojejunal anastomosis	4 Pigs	Stents degraded completely after 3 months, the anastomosis had no obvious abnormality and its diameter was larger than the control.	[78]
PLA	7 mm	Benign biliary Strictures	9 Pigs	Stents degraded completely and had good patency at 6 months. Compared with covered SEMS, PLA stents may bring proteins expression towards which was seen in intact bile duct.	[35]
PLLA	–	Duct-to-duct anastomosis	4 Dogs	Bile duct patency was good at 3 months with no significant complications.	[37]
PLLA	6 mm	Normal bile duct	12 Dogs	No blockage or stent migration occurred, and stent degradation was evident at 9 months.	[79]
PLGA	0.98 mm	CBD	80 Rats	Stents disappeared spontaneously within 4–5 weeks without serious complications.	[43]
PLGA	10 mm	CBD	6 Dogs	The stents had the desired biomedical properties and automatically disappeared from the CBD within 4–5 weeks.	[44]
PDX	10 mm	Benign intrahepatic biliary strictures	2 Patients	As a result of the exclusion of stent fragments after 3 months, patients developed transient cholangitis and were asymptomatic 2 years later.	[46]
PDX	8–10 mm	Benign biliary Strictures	10 Patients	With a median follow-up of 16.5 months, there was no sign of biliary stricture or dilatation, and the stents were completely degraded within 6 months.	[47]
PDX	8 mm	Hepaticojejunostomy biliary leak	1 Patient	The stent was able to drainage well and the sepsis had been resolved.	[48]
PDX	8 mm	Benign biliary Strictures	107 Patients	At a mean follow-up of 23 ± 12 months, no major complications occurred and there were 2 cases of stent migration, 4 cases of mild haemobilia and 19 cases of restenosis.	[49]
PDX	8 mm	Cystic duct leak	1 Patient	Patient was in good condition with no leakage or inflammation after 7 days, the stent underwent the expected degradation at 6 months.	[50]
PDX	10 mm	Benign biliary stricture	1 Patient	The stent completely disintegrated at 5 months, leading to collapse of the stenosis, which in turn caused persistent obstruction.	[51]
PDX	10 mm	CBD	23 Pigs	Presence of mild-moderate inflammatory response, stents absorbed completely within 13–20 weeks.	[52]
PDX	2–4 mm	Biliary complications after LT	12 Patients	After a median follow-up of 13 months, four patients developed biliary complications, including biliary fistula, biliary leak and stricture.	[53]
PDX	–	Duct-to-duct biliary anastomosis.	5 Patients	Stents showed anticipated degradation with good biliary patency and there was no evidence of bile leakage or stone formation.	[54]
PDX	10 mm	Hepaticojejunostomy strictures	13 Patients	Two patients developed cholangitis and biliary stricture at a mean follow-up of 20 months, respectively.	[55]
PDX	8 mm	Benign biliary strictures	2 Patients	During 6 months of follow up, the stents showed the expected degradation, which appeared to be sufficient to remodel and eliminate the strictures.	[56]
PDX	8–10 mm	Benign biliary strictures Cystic duct leaks	13 Patients	All bile leaks were resolved, the clinical success rate for the treatment of benign biliary strictures was 83 % in a median follow-up of 21 months.	[57]
PDX	6–10 mm	Biliary strictures after LT	20 Patients	Three patients (two adults and one child) with anastomotic stenosis had recurrence of the stenosis after 3, 7 and 25 months.	[58]
PDX	10–12 mm	Benign biliary anastomotic strictures after LT	18 Patients	After a median follow-up time of 27.2 months, complete relief of anastomotic stricture was achieved in 72 % of patients.	[59]
PCL	3 mm	Bile duct	4 Pigs	The stents can be successfully placed in the bile ducts and dilation achieved.	[65]
PVA	–	Bile duct	1 Pig	The stent enlarged the bile ducts effectively without interfering with the flow of bile.	[71]
PGA	10 mm	Bile duct	-, Pigs	Stents degraded rapidly and disappeared completely within 4 weeks.	[73]

PLA: polylactide; PLLA: poly (L-lactic acid); PLGA: poly (lactic-co-glycolic acid); PDX: polydioxanone; LT: liver transplantation; CBD: common bile duct; Covered SEMS: covered self-expandable metal stent.

PDX: polydioxanone; CSEMS: covered self-expandable metal stent. PDX: polydioxanone; PCL: polycaprolactone; PVA: poly (vinyl alcohol); PGA: polyglycolide; LT: liver transplantation.

3.2. PDX-based stents

PDX is degraded to small molecules in the body and then metabolized. It has been used for the manufacturing of biodegradable medical devices [45], also used in the preparation of biliary stents. PDX stents are usually labeled with radiopaque gold or platinum to facilitate observation of stent degradation and recovery of biliary strictures after implantation. PDX-based stents are currently the most widely studied biodegradable biliary stents with the largest number of clinical trials and the longest follow-up. These stents are used for managing bile leaks, bile duct anastomosis, benign biliary strictures, etc. and were biocompatible with no significant complications, and completely degraded after a few months [46–59]. Recently, PDX-based Archimedes stents have been designed for endoscopic application, Fig. 2M. This stent has a unique helical geometry that is thought to promote the flow of bile on the outer surface of the stent while supporting the opening of the bile duct [60]. By adjusting the composition, these PDX-based stents have two different degradation rates: fast and medium, with degradation times of 12 and 20 days, respectively. Anderloni et al. [60] preliminarily found that these stents degraded in the patients' bile ducts as expected and were technically successful in various indications. However, the mechanical properties of PDX are inferior and its Young's modulus is comparatively low [3]. The degradation product may acidify the local environment, which could trigger a potentially proliferative response in the bile duct [61]. These drawbacks may limit the use of PDX stents for complex biliary strictures.

3.3. PCL-based stents

Structurally stable, non-toxic, and biodegradable, PCL is extensively used for biomedical applications such as nanocarriers and stent materials [62,63]. Tashiro et al. [64] prepared stents from a copolymer of lactic acid and caprolactone for duct-to-duct biliary reconstruction. At 180 days post-implantation, the stents were essentially completely degraded, with good patency and only slight chronic inflammation and fibrosis in the anastomotic region. Itoi et al. [65] successfully implanted PCL stents into porcine bile ducts, and subsequent necropsy revealed that the stents had dilated [65]. But histological analysis and long-term evaluation are lacking. Nevertheless, PCL is still mainly used as a coating material for stent. Recently, PCL has become the most favored polymer for extrusion-3D printing due to its 55–60 °C melting temperature [66]. However, the poor mechanical properties and slow degradation rate (2–4 years) of PCL are still the main reasons for the limitation of its medical application [67].

3.4. PVA-based stents

PVA is a synthetic biodegradable polymer that can mimic native polymers and exhibits exceptional biocompatibility in human tissues [68]. Hydrogels based on PVA (PVA-hydrogels) are colloidal dispersion, which crosslink and swell to form three-dimensional networks. PVA-hydrogels have received much attention in the biomedical applications such as healing products, tissue engineering stents, and drug delivery carriers due to their excellent biocompatibility, low toxicity, high water absorption, and good mechanical properties [69]. Nagak et al. [70] pioneered the use of hydrogels as a new concept for SEMS. They ingeniously exploited the water-absorbing and swelling properties of PVA-hydrogels to prepare an especially SEMS. The dried tubular PVA-hydrogels exhibited an isotropic 1.4–1.5-fold increase in the ratio of inner and outer diameter and length in physiological saline. In addition, the radial force of the reswollen tubular PVA-hydrogels was remarkably greater than that of the conventional metal stent (6.6 ± 0.6 mN mm^{-2} vs 4.4 ± 0.3 mN mm^{-2}). This result suggested that PVA-hydrogels can be applied to SEMS. Then, they successfully delivered the PVA-hydrogels stent into the porcine bile duct via endoscopy and found that the stent effectively dilated the bile duct without interfering with the flow of bile. Four weeks after implantation, the stent patency was good, but protein was present on the stent surface [71]. Adhesion of host proteins is the preliminary stage of biofilm formation, and 4 weeks of implantation is too short for biofilm formation. Therefore, it remains to be seen whether the stent can effectively inhibit biofilm formation over a longer period of time.

3.5. PGA stents

PGA is considered to be a clinically acceptable, readily available, processable material with known biological responses and is therefore used in tissue engineering and regenerative medicine [72]. Kwon et al. [73] observed morphological changes in PGA stents at 6 weeks and complete degradation at 8 weeks in vitro bile flow phantom model. However, the PGA stents degraded rapidly in the porcine bile ducts, with the fragments completely disappearing within 4 weeks. The PGA stents can achieve short-term support of the bile ducts, but for long-term support, the corrosion rate needs to be retarded. In addition, the biological response of PGA stents to biliary tissue remains to be elucidated.

Overall, biodegradable polymer stents have significant advantages over traditional non-biodegradable stents, but there are also the following issues. One of the prominent issues is the poor mechanical properties of biodegradable polymer stents, followed by biocompatibility, and support time of the stent, as presented in Table 2. Due to the poor mechanical properties of polymers, it is necessary to increase the thickness of the polymer filaments used to braid the stent in order to achieve sufficient radial force [74]. This will take up more lumen area and may interfere with bile flow. In addition, as the contact surface of this stent with the biliary tissue is increased, it may increase the risk of a hyperplastic reaction and restenosis [74]. Improving the mechanical properties of these polymers has been a hot issue in research. The following are effective ways to improve the mechanical properties of PLA, PLLA, PDX, and PCL, mainly by doping with mechanically enhanced substances and optimizing the manufacturing technology. The mechanical properties of PLA can be enhanced by blending it with.

other materials such as zeolite [80], polyethylene glycol (PEG) [81]. The stiffness of the PLA matrix was increased by 21.48 % compared to the PLA without zeolite incorporation [80]. A biliary stent made

from PLA-b-PEG-b-PLA triblock copolymer has mechanical properties comparable to those of the silicone stent currently used in liver transplantation [81]. Furthermore, the tensile strength (336.1 MPa) and Young's modulus (4.1 GPa) of PLA fibres produced using the novel Versatile Disorder-to-Order technology were 5.2 times and 2.1 times higher, respectively, than those produced using the spinning method [82]. Such excellent mechanical properties even exceed those of some metals (e.g., magnesium alloys) and are highly desirable for use in biliary stents.

Regulation of the molecular weight, adjustment of crystallization, and controlling of crack propagation of PLLA are important approaches to enhance its mechanical properties [83]. The molecular weight of PLLA can be adjusted by grafting joncryl onto the PLLA molecular chain. Modified PLLA showed higher tensile strength, toughness, and strain at break than unmodified PLLA [84]. Adjusting crystallinity is considered one of the most effective ways to improve the mechanical strength of PLLA [85]. Silanated cellulose nanocrystals (SCNC) offer excellent nucleation on PLLA via strong hydrogen bonding. The crystallinity of PLLA was effectively increased by 112.6 %, and the tensile strength and tensile modulus were improved by more than 20 % after the addition of 1 wt% SCNC [86]. The zeolite imidazolate framework (ZIF-8) has favorable stiffness and facilitates nucleation of PLLA [87]. ZIF-8 was introduced into PLA scaffolds using selective laser sintering, and the tensile and compressive strengths of the scaffolds were increased by 36.9 % and 85.6 %, respectively, after the incorporation of 2 wt% of ZIF-8 [88]. The introduction of the reinforcement phase into the PLLA matrix can alter the crack growth path of created fracture area, thus increasing toughness by consuming more fracture energy [83]. For this

Table 2
Characteristics of typical biodegradable biliary stents.

Materials	Mechanical properties			Degradation period*	Main disadvantages	Ref
	TS(MPa)	YM (GPa)	EL (%)			
PLA	88	8.6	30	<6 months	Poor mechanical properties, acidic degradation products	[35,118]
PLLA	40–60	2–5	2–10	>9 months	Slow degradation rate, acidic degradation products	[38,83]
PLGA (71:29)	–	–	–	4–5 weeks	Fast degradation rate, acidic degradation products	[43,96]
PCL	25–30	0.2–0.4	700–900	–	Poor mechanical properties, slow degradation rate	[65,83]
PDX	–	–	–	<6 months	Poor mechanical properties, acidic degradation products	[3,47,61]
PGA	60–99.7	6–7	1.5–20	<4 weeks	Fast degradation rate, acidic degradation products	[73,83]
Mg alloy	220	44	2	>3months	Fast degradation rate, hydrogen gas generation	[115,119,120]

PLA: polylactide; PLLA: poly (L-lactic acid); PLGA: poly (lactic-co-glycolic acid); PCL: polycaprolactone; PDX: polydioxanone; PGA: polyglycolide; Degradation period*: refers to the degradation period of the material in the bile duct.

purpose, a number of inorganic reinforcing phases (e.g. whisker and fibers) are added to PLLA to control crack propagation behavior [83]. In addition, some organic ductile polymers can also enhance the toughness through polymer blend. For example, the elongation at break of PLLA increased from 8.9 % to 256 % when poly (vinylidene fluoride) and reactive graft copolymer were added [89].

The incorporation of reinforcing elements such as chitosan (CS) can significantly enhance the mechanical properties of PDX. The highest tensile strength and Young's modulus of the PDX/CS blended films, 32.75 MPa and 1108 MPa, respectively, were obtained when the chitosan content was 30 wt% [90]. Furthermore, adjustment of annealing temperature and annealing time could also improve the mechanical properties of PDX [91].

Reinforcing PCL with cellulose nanofillers can improve its mechanical properties [92]. With the addition of only 0.2 wt% of nanofibrillated cellulose, the elongation at break, tensile strength, and impact strength of PCL were increased by about 38 %, 27 % and 38 %, respectively [93]. Hashim et al. [92] grafted nanofibrillated bacterial cellulose onto PCL and the nanocomposites with 13 wt% cellulose content were the stiffest films with ultimate strength and Young's modulus of 57.3 MPa and 661.3 MPa respectively. These pathways are effective in improving the mechanical properties of the polymers, and the resulting stents may have even better mechanical properties to support the bile ducts. However, whether these modified polymers are sufficiently biocompatible remains to be demonstrated.

Although these polymer stents possess acceptable biocompatibility, their (e.g., PLA [94], PLLA [95], PLGA [96], and PDX [61]) degradation process generates a large number of acidic products, which may lead to a decrease in the pH of the local environment, thus inducing a potential inflammatory response. One feasible resolution is the addition of a neutralizing agent to counteract the acidic degradation products produced by the polymer. The incorporation of magnesium [97–100], magnesium oxide [101–103], magnesium hydroxide [104–107], magnesium fluoride [100], calcium citrate [108], etc. into the polymers effectively neutralizes the acidic environment generated by the degradation of the polymers, thus improving the biocompatibility of the polymers. The incorporation of these alkaline particles is expected to neutralize the local acidic environment produced by the polymer-based biliary stents, thereby mitigating the corresponding complications.

Biliary stents require appropriate support time to remodel strictures. However, the optimal duration of stenting for durable remodeling of benign biliary strictures remains uncertain. In most studies, the duration of treatment ranged from 3 to 12 months [2]. Most existing biodegradable biliary stents (including Mg-based alloy stents) are not yet adequate for such long support time. There is a need to increase the corrosion resistance in view of this need for long-term support. Conversely, degradation period that are excessive, e.g., PLLA (18–36 months), PCL (24–36 months), do not satisfy biliary repair requirements and need to be accelerated [83]. Researchers could use surface modifications, polymer blends, and incorporation of alkaline particles to accelerate PLLA degradation [83]. Copolymerization of PCL with lactide, glycolide, δ-valerolactone, and ethylene oxide could accelerate the degradation rate [109]. For specific conditions such as choledocholithiasis, acute cholangitis, and other anatomic T-tube indications, placement of a T-tube is required to provide mechanical support and drainage [110]. However, T-tubes are composed of nonbiodegradable materials (e.g., red rubber, silicone, polyvinyl chloride, and latex) and are typically left in place for 7–21 days with a complication rate of 2 %–6 % [111]. Therefore, PLGA and PGA are suitable alternatives to T-tubes. But they need to be incorporated with alkaline substances to counteract the acidic products generated during their degradation. A suitable degradation rate with enhanced mechanical properties and alkaline components remains issues to be addressed in existing biodegradable polymer stents.

3.6. *Magnesium alloy-based stents*

The biocompatibility and degradation behavior of magnesium (Mg) alloys were intensively studied in cardiovascular stents [112], providing insight into their applicability as biliary stents. Chen et al. [113] showed that one-week post-implantation of the Mg-6Zn stents, a large portion of the stents remained in the rabbit bile duct. After three weeks, the residual stent weight was only 9 % of the original weight. They further found that low concentrations of Mg-6Zn alloy extract induced apoptosis of biliary epithelial cells, while high concentrations may promote necrosis or 'apoptotic necrosis'. However, apoptotic bodies and cell necrosis were not observed in the periprosthetic tissue [114]. This phenomenon may be associated with a reduced corrosion rate in vivo and localized concentrations of Mg^{2+}. Liu et al. [115] implanted AZ31 stents into the common bile duct (CBD) of rabbits. The residual stent volume was 93.82 ± 1.36 % of the original at 1 month and 30.89 ± 2.46 % at 3 month, respectively, and the inflammation was restored to normal levels. Currently, the UNITY-B stent made from Mg alloy ($MgNdMn_{21}$) has received CE approval for the treatment of biliary strictures, Fig. 2L. A clinical trial assessing the security and efficacy of this stent also revealed a high success rate of 94.4 % [3].

Palliative treatment of malignant biliary strictures with stent is temporary because stents cannot inhibit tumor growth. Recently, researches confirmed that Mg strongly inhibited the growth of gallbladder cancer cells and cholangiocarcinoma cells in vitro. In tumor-bearing mice, the tumor size and weight were significantly reduced [116,117]. This suggested that the Mg-based stents are likely to be suitable for patients with biliary strictures caused by cancers. While providing support and drainage, the stent may also be effective in inhibiting tumor growth, thereby prolonging patient survival. These studies indicated that Mg alloys were biocompatible in the bile ducts. However, the excessive degradation rate of Mg alloys, leading to premature loss of mechanical support of the stent is the main reason limiting its clinical application.

In conclusion, the performance of biodegradable biliary stents is acceptable but still lacks long-

lasting supportive capacity and adequate in vivo evaluation. Besides the radial forces, it is important to note that the axial forces (AF). The AF should be relatively low, as stents with higher AF may not fit or be stable

in the bile ducts, thereby damaging the bile duct wall and leading to biliary sludge, migration, and cholangitis [121]. It is worth mentioning that the metal zinc (Zn) has created a wave of research in the field of degradable metal stents owing to its suitable degradation rate (between iron and Mg), fracture strength, elongation, and biocompatibility [122]. Zn-based stents maintained long-term support in vascular (approximately 6 months) without inflammatory reactions and thrombosis [123]. Moreover, zinc oxide particles, one of the main degradation products of Zn alloys, possess multiple biological functions such as anticancer, anti-inflammatory, and antibacterial properties [124]. From the above, Zn and its alloys are excellent candidates for the manufacture of biliary stents. Unfortunately, studies on Zn and its alloys for biliary stents have not yet been reported.

4. Surface modification of biliary stents

Biliary stents provide only basic mechanical support without biological functions. These stents seem powerless when confronted with in-stent restenosis due to tumor growth, biofilm formation, and tissue hyperplasia [6,7]. Consequently, over the past two decades, functional coatings have been created for biliary stents to prolong stent patency. According to their functions, these coatings are primarily classified as antitumor coatings, stone-dissolving coatings, antibacterial or anti-biofilm coatings, antiproliferative coatings, and corrosion-resistant coatings, as shown in Fig. 4. Coating preparation techniques commonly used for biliary stents (including dip coating, electrospinning, covalent immobilization, layer by layer, and electrophoretic deposition) have also been presented in Fig. 5.

4.1. Antitumor coatings

Cholangiocarcinoma (CCA) is a malignant tumor derived from bile ducts [125]. There are no specific early clinical indications due to the high heterogeneity of CCA. Unresectable, locally advanced, or metastatic disease is diagnosed in the bulk of patients [126]. Stent implantation is a palliative option for drainage and to improve patients' quality of life [127]. However, tumor ingrowth or overgrowth often leads to in-stent restenosis. Therefore, the loading of antitumor agents on biliary stents may be a very promising treatment for malignant biliary strictures. In addition, local drug delivery systems based on stents also allow for the controllable release of therapeutic drugs to specific tissue sites, thereby increasing the site-specific efficacy and minimizing the systemic toxicity [128]. Antitumor agents such as carboplatin (Car) [129], paclitaxel (PTX) [130,131], gemcitabine (GEM) [132], sorafenib (Sor) [133], vorinostat (Vor) [134] were used for manufacturing the antitumor coatings.

The antitumor activities of these coatings in vitro and in vivo have been well established and are presented in Table 3.

Tumor cell-specific microenvironment e.g., reactive oxygen species (ROS) and pH, offers the possibility for responsive and precise release of drugs from coatings. ROS expression is upregulated in cholangiocarcinoma cells [135], which could be exploited to achieve drug-specific release, thereby reducing lateral effects. Jang et al. [136] showed that piperlongumine (PL)-PCL-LEse coatings accelerated PL release in the presence of H_2O_2. The PL-PCL-LEse membrane also induced ROS production in HUCC-T1 cells and enhanced apoptosis. After 40 days of implantation in tumor-bearing

Mice, the tumor volume was significantly suppressed in the PL-PCL-LEse group than in the other groups.

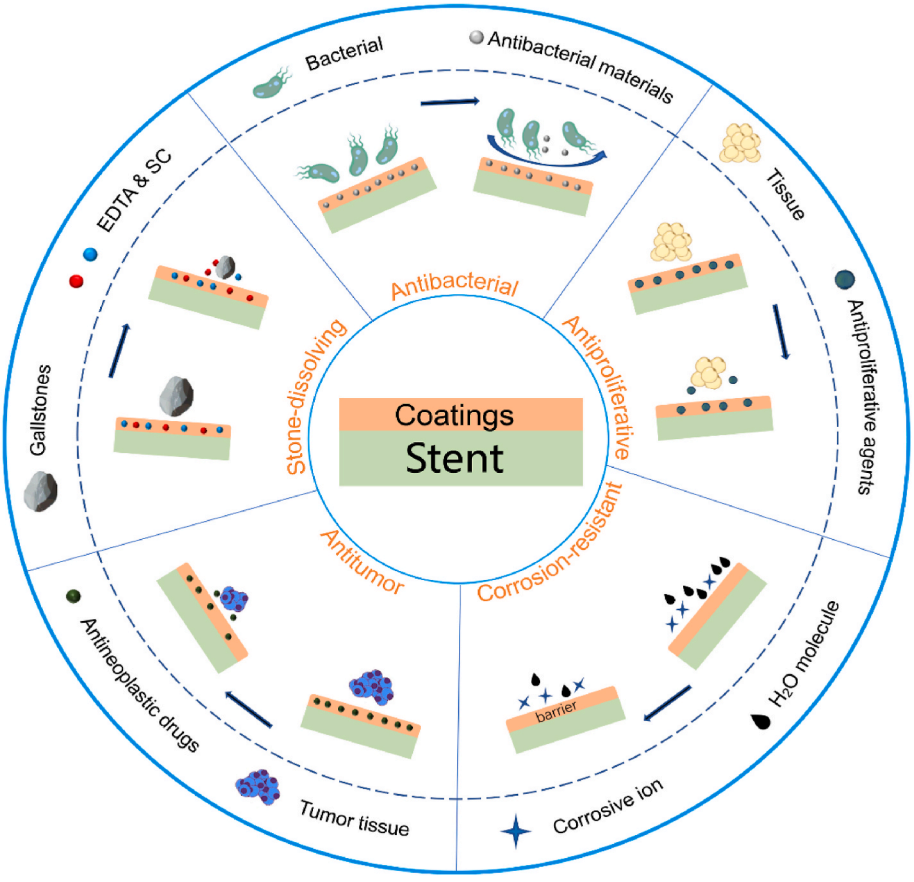

Fig. 4. Typical functional coatings of biliary stents.
EDTA: ethylenediaminetetraacetic acid; SC: sodium cholate.

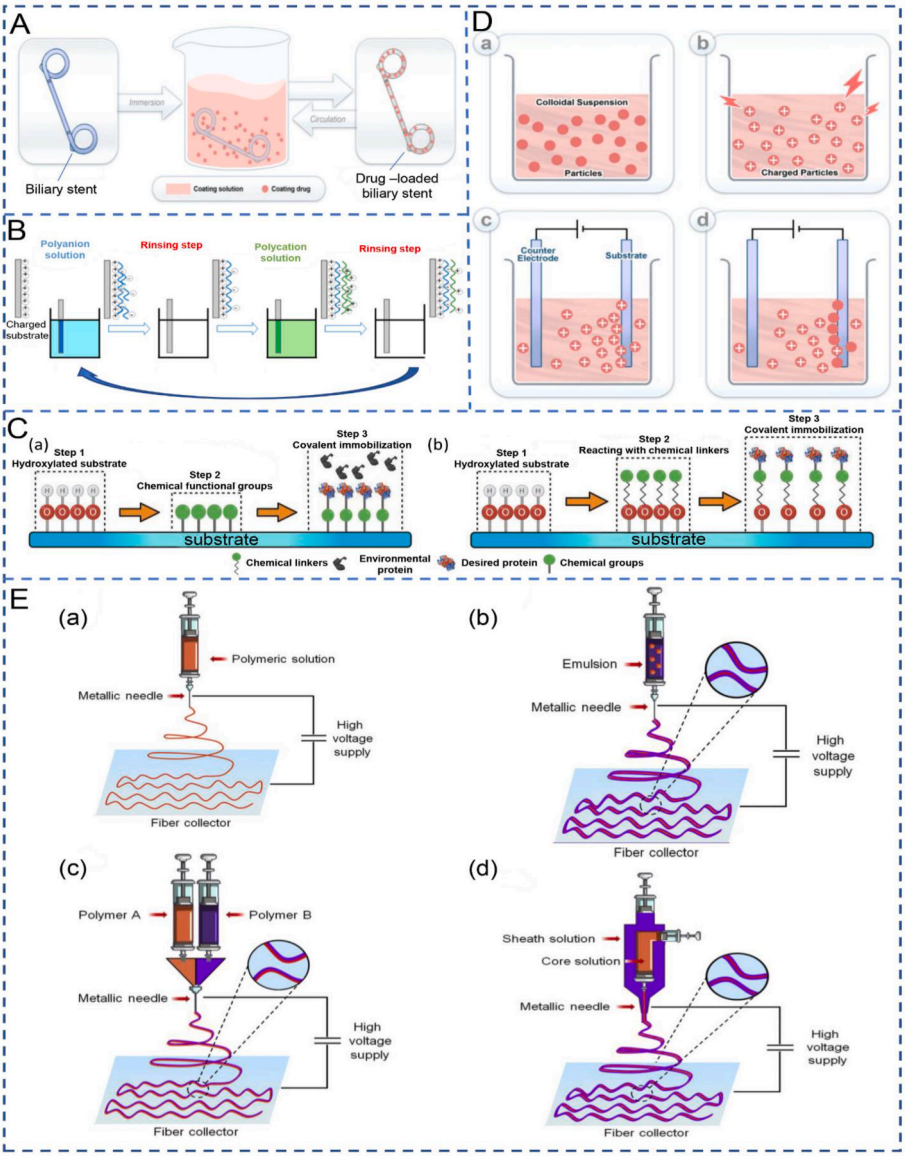

Fig. 5. Coating preparation techniques commonly used for biliary stents. A: Dip coating. B: Layer by layer [137]. **C:** Covalent immobilization [138]. (a): Direct covalent immobilization through wet chemical methods. (b): Covalent immobilization using chemical linkers. **D:**Four steps of electrophoretic deposition [139]. (a) dispersion, (b) electrochemical charging, (c) electrophoresis and (d) deposition. **E:** Schematic illustration of four electrospinning methods [140]. (a) Single nozzle electrospinning. (b) Single nozzle electrospinning with emulsion. (c) Side-by-side nozzle electrospinning. (d) Coaxial nozzles electrospinning.

The above coatings contain only one drug, and the combination of GEM and cisplatin (CIS) is currently the standard chemotherapy protocol for treating CCA [126]. Xiao et al. [141] prepared stent coatings with different GEM & CIS contents by mixed electrospinning, Fig. 6A. In the mice tumor xenograft model, antitumor activity of the 10 % drug-eluting membranes was superior to single and no

Drug-contained coatings, as shown in Fig. 6B and C. Moreover, after 4 weeks of implantation of the coated stent into the porcine CBD, no significant abnormal changes were observed in the bile duct.

Despite designing a drug-releasing stent and placing it near the target, only a small portion of the agent delivered from the coating reached the lesion, because the drug also acted on surrounding normal cells [142]. Therefore, drug carriers that can bind specifically to the target allows for efficient and accurate drug delivery to the lesion. Yun et al. [142] constructed GEM & PTX-containing nanoparticles (TCMPNs), in which hyaluronic acid promoted the endocytosis of nanoparticles by interacting with.

The CD44 receptor of CCA cells. After 30 days of implantation of the drug-eluting membrane into mice, the TCMPNs-containing group showed a significant reduction in tumor volume and weight compared to the other groups.

Currently, antitumor coatings are far from ideal for clinical use. Due to technical limitations, there is a lack of suitable animal models of CCA. A considerable number of antitumor assessments were performed in tumor xenografts, that do not genuinely reflect malignant biliary strictures.

4.2. *Stone-dissolving coatings*

Endoscopic sphincterotomy is the standard treatment for CBD stones [143]. However, 10 %–15 % of stones cannot be retrieved due to excessive number, large size, among others [144]. Endoscopic temporary placement of a biliary stent is recommended for patients with unretrievable CBD stones

That require biliary drainage. Biliary stents can also break up large stones, allowing them to pass out spontaneously or be extracted more

Table 3
Antitumor coatings.

Substrate	Coating			Evaluation			Ref
	Medicine	Material	Technique	In vitro	In vivo	Main result	
PU tube	Car	Car-PVA/PU	Dip coating	HuCC-T1	HTBM Patients	The coated tubes significantly inhibited the cancer cell growth and the tumors size was reduced in mice. In 5 patients with coated tubes, the overall rate of effectiveness was 60 %.	[129]
NITI-S	PTX	PTX-PU	Dip coating	–	Pigs	Coated stents were safe, but there existed fibrous reactions and inflammatory cell infiltration in the bile duct.	[130]
NITI-S	PTX	PTX-Plu-PU	Dip coating	SK-Cha-1	Pigs	The coated stents were safe, but presented inflammatory and fibrotic reactions.	[131]
Metal stent	GEM	GEM-PU-PL[a]	Dip coating	SK-Cha-1	–	GEM-PU-PL12 % effectively inhibited cancer cell proliferation and strongly induced pro-inflammatory cytokines and p38 MAPKs.	[132]
Metal stent	Sor	Sor-PCL	Electrospinning	HuCC-T1	HTBM	Sor-PCL film effectively inhibited proliferation, angiogenesis, and invasion of cancer cells.	[133]
GI stent	Vor	Vor-PLGA	Electrospinning	Multiple cells	HTBM	Vor-PLGA coatings exhibited marked antitumor activity against CCA cells.	[134]
GI stent	PL[b]	PL-PCL-Lese	Electrospinning	Multiple cells	HTBM	The coating exhibited ROS responsiveness and induced ROS production in tumor cells, showed good antitumor activity.	[136]
Covered metal stent	GEM CIS	GEM &CIS-PLCL/PLCL	Electrospinning	EGI-1	ETBM Pigs	The drug-eluting membranes effectively inhibited tumor growth, and the coated stents can be used safety in porcine bile duct.	[141]
Covered metal stent	TCMPNs	TCMPNs-PU	Dip coating	HuCC-T1 SCK	HTBM	TCMPNs-PU films significantly inhibited cancer cell growth compared to the other groups.	[142]

Car: carboplatin; PTX: paclitaxel; GEM: gemcitabine; CIS: cisplatin; Sor: sorafenib; Vor: vorinosta; PL[a]: poloxamer 407; PL[b]: piperlongumine; TCMPNs: temporally controlled polymeric multi-prodrug nanoparticles; PU: polyurethane; PLGA: poly (lactic-co-glycolic acid); PVA: poly (vinyl alcohol); PCL: polycaprolactone; PLCL: poly-L-lactide-caprolactone; Plu: Pluronic F-127; Multiple cells: HuCC-T1 CCA, SNU478, SNU245, SNU 1196; HTBM: HuCC-T1-tumor bearing mice; ETBM: EGI-1-tumor bearing mice; CCA: cholangiocarcinoma. ROS: reactive oxygen species.

easily later [145]. For efficient reduction of stone size and facilitation of stone elimination, several studies have investigated the effectiveness of stone-dissolving drugs [ethylenediaminetetraacetic acid (EDTA) and sodium cholate (SC)] loaded onto biliary stents [146–150]. Cai et al. [147] placed stents coated with different levels of EDTA and SC together with stones in porcine bile ducts, Fig. 7A. The coated stents were biocompatible, Fig. 7C. After 6 months, all stones were reduced in weight, with the 50 % EDTA & SC-coated stent group losing more weight than the no coatings and 0 % coatings (269 ± 66 mg vs. 179 ± 51 mg [P = 0.09]; 269 ± 66 mg vs. 156 ± 26 mg [P = 0.01], respectively), Fig. 7B.

These coatings offer a novel idea for assisting in the extraction of difficult-to-remove CBD stones, but their effectiveness in dissolving stones remains to be improved, as shown in Table 4. The flow of bile could accelerate the loss of drug-containing coatings, and enhancing the stability of the coatings as well as maintaining a high concentration of the drug around the stones may increase its efficiency in dissolving the stones. Besides, CBD stones mainly include cholesterol stones, black pigment stones, and brown pigment stones [151]. Cholesterol stones are mainly made up of cholesterol monohyd-rate, polymerized calcium bilirubinate is the main component that forms black pigment stones, while brown pigment stones are composed of a mixture of calcium salts of long-chain fatty acids and cholesterol [152]. The above studies did not include different types of stones, and the shape, size, location and number of stones, are also factors worth considering.

4.3. Antibacterial or antibiofilm coatings

Bacterial infection, the formation of biofilm, and cholestasis usually lead to recurrence of stones post ERCP [153]. This was explained by the fact that the implantation of the stent interfered with bile kinetics and was more likely to result in concentration of bile and consequent cholestasis [154]. The concentrated bile was able to stimulate inflammatory changes in the biliary mucosa and increased the concentration of calcium, unconjugated bilirubin, bile acid, and glycoproteins, promoting the development of stones [153]. In particular, dysfunction of the sphincter oddis and reduced pressure in the bile duct after stent implantation led to bacterial reflux from the duodenum into the bile duct, which can cause secondary infections and occlusion [155,156]. Therefore, avoiding reflux of duodenal contents is the key to eliminating stone recurrence. Anti-reflux systems equipped at the duodenal end of biliary stents have been recognized as a potential solution to reduce reflux, effectively minimizing the complications caused by reflux [157,158], Fig. 8. However, there is still a risk of poor bile drainage and obstruction [159].

As an alternative, stent patency can be prolonged by preventing biofilm formation caused by reflux. Biofilm formation mainly involved four steps [160]: I) Reversible attachment: bacteria attach to substrate via cell pole or flagellum, with subsequent longitudinal attachment. II) Irreversible attachment: the switch to irreversible attachment is accompanied by the generation of biofilm matrix components, reduction in flagella reversal rates, and decrease in flagella gene expression. III) Biofilm maturation: the presence of cell clusters that several cells thick embedded in the biofilm matrix (Maturation I), which then fully mature into microcolonies (Maturation II). IV) Dispersion: the reduction and degradation of matrix components, with dispersed cells being motile, Fig. 9. The biofilm effectively prevent the internal bacteria from immune system and also limit the efficacy of antibiotics [161]. This suggested that conferring resistance to protein adsorption and bacterial adhesion on the stent surface to prolong patency is feasible. Currently, silver nanoparticles (AgNPs), sulfonic acid groups contained substances, antibiotics, chitosan, etc., have been used to prepare antibacterial or antibiofilm coatings. The antibacterial effects of most coatings are reviewed in Table 5.

4.3.1. AgNPs-related coatings

AgNPs possess antimicrobial, anti-inflammatory, antiviral, and antioxidant properties, and are used in medicine to prevent infections [162].The strong antibacterial activity of AgNPs in vitro and in vivo have been demonstrated in several studies, which could be used to prevent bacterial infections in biliary stents [163–166], as shown in Table 5. For malignant biliary obstruction, radiofrequency (RF) ablation combined with SEMS has been demonstrated superior clinical outcomes compared to stenting alone [167,168]. However, bacterial colonization, which may raise the risk of sepsis and inflammatory response, is linked to this combination [169]. Park et al. [170] prepared the AgNPs/PDA-coating on SEMS (Fig. 10), which suppressed stent-induced tissue hyperplasia and the formation of biliary sludge. They further demonstrated that the AgNPs/PDA-coated stents combined with RF were sufficient to reduce tissue hyperplasia, thermal damage, and the growth of bacteria in rabbits [169], Fig. 10B and C.

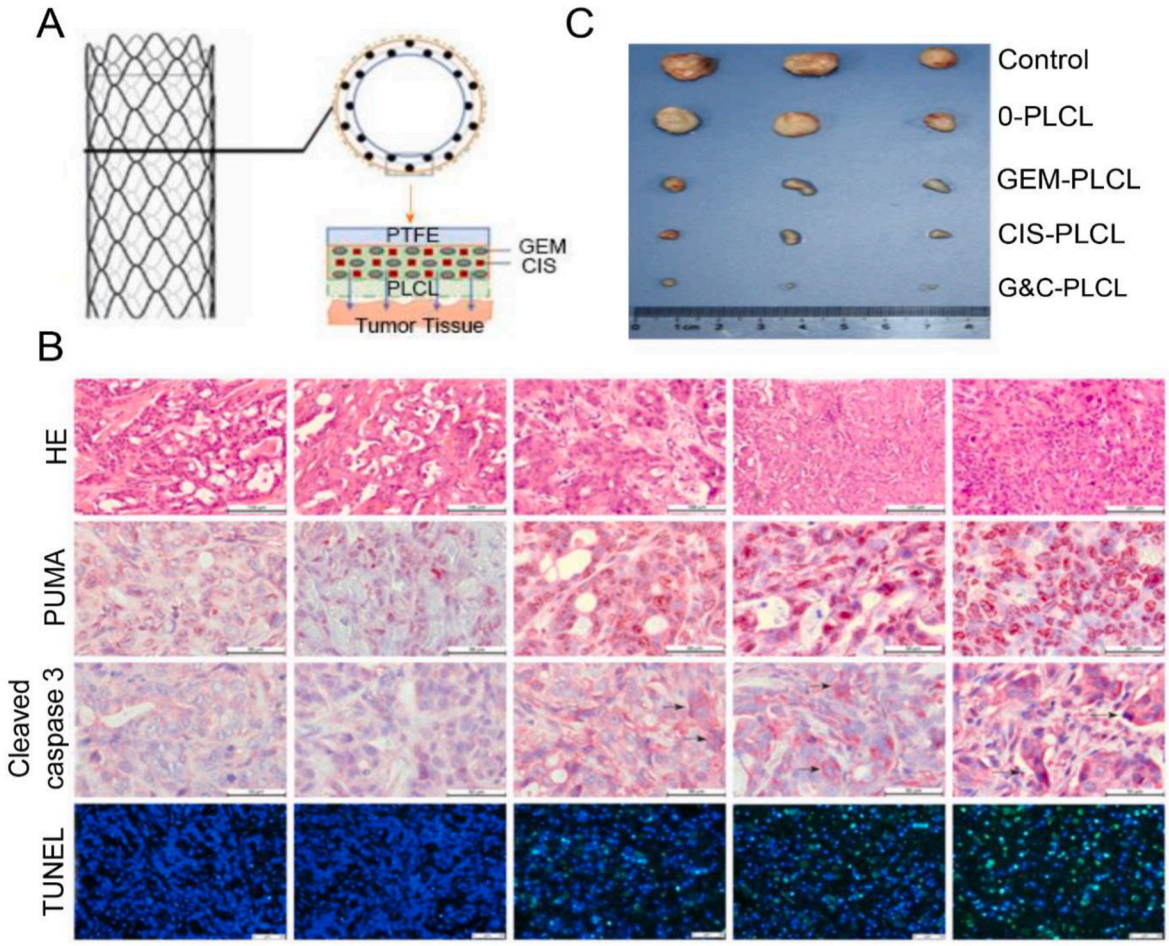

Fig. 6. Antitumor activity of GEM & CIS coatings in vivo [141]. **A:** Schematic diagram of the coated stent. The inner, middle and outer layer of the coating is PTFE membrane (as a barrier to prevent drug loss), PLCL layer (as the primary drug carrier), and PLCL-unloaded outer membrane (as a barricade to avoid burst release), respectively. **B:** HE staining (× 200, 100 μm scale bar), immunohistochemical detection of p53 upregulated modulator of apoptosis and cleaved caspase-3 (× 400, 50 μm scale bar), and terminal deoxynucleotidyl transferase-mediated dUTP nick end labeling (× 200, 50 μm scale bar) in subcutaneous tumor tissues. **C:** Subcutaneous tumors in nude mice after 4 weeks of drug-loaded nanofilm implantation. PTFE: polytetrafluoroethylene; GEM: gemcitabine; CIS: cisplatin; HE: hematoxylin and eosin; PLCL: poly L-lactide-caprolactone; PUMA: p53 upregulated modulator of apoptosis; TUNEL: terminal deoxynucleotidyl transferase-mediated dUTP nick end labeling.

Nevertheless, the potential biosafety issues of AgNPs need to be taken seriously. Ingested AgNPs are distributed to various organs and tissues, for example the hepatobiliary, nervous, and urinary systems. These deposited AgNPs may cause genetic mutations, apoptosis, or cell necrosis that are possibly toxic to tissues or organs [171]. The possible cytotoxicity of AgNPs is determined by the available concentration and size of AgNPs, the pH of the environment, the duration of the activity, the presence or absence of stabilizer, and the type of stabilizer [172].

Controlling particle size, surface functionalisation and compound preparations as potential methods to overcome cytotoxicity of AgNPs. The cytotoxicity produced by silver nanoparticles of different particle sizes varies for different cells [173,174]. The EC_{50} values of rat cortical neurons treated with AgNPs with diameters of 20 nm and 70 nm for 24 h were 6.61 ± 0.28 μg/mL and 38.4 ± 1.61 μg/mL, respectively [173]. This may be due to the fact that smaller silver nanoparticles are more readily taken up by cells and cause greater toxicity [175]. Cytotoxicity of PEG-coated and bovine serum albumin-functionalized AgNPs is significantly attenuated compared to unmodified AgNPs [176]. In addition, the cytotoxicity induced by silver nanocomposites, e.g., AgNPs/carboxymethyl cellulose composite [177], AgNPs–porous slicon mcroparticles [178], cellulose nanofibrils/AgNPs complex.

[179], was also significantly reduced. These factors need to be taken into account for the design of.

AgNPs-coatings used in medical applications.

4.3.2. *Sulfonic acid groups contained substances*

Materials containing sulfonic acid groups, such as heparin (Hep) and sulphated hyaluronic acid, are used for surface modification of medical devices to impart antibacterial feature [180,181]. Cetta et al. [182] cultured sulfonated hyaluronic acid coated PUPA with bacteria isolated from clogged stents.

The bacterial adhesion on coated surface was reduced compared to the uncoated surface. Similarly, Peng et al. [183] showed that the sulfonated PE tube could effectively reduce the adhesion of *E. coli* in human bile. In a prospective randomized trial, patients were treated with Hep-polyethyleneimine-coated stents and native stents for nearly 3 months [184]. The results showed that the mean encrustation weight of the native stent was more than twice that of the coated stents (native: 37.9 ± 19.8 (16–93) mg; coated: 17.6 ± 6.7 (9–33) mg). Nonetheless, this is a preliminary study, and it remains to be demonstrated whether it could prolong the stent patency by inhibiting stent occlusion, thereby reducing

The number of ERCP procedures.

4.3.3. *Hydrophilic or hydrophobic coatings*

Wettability is an important property of solid surface that influences

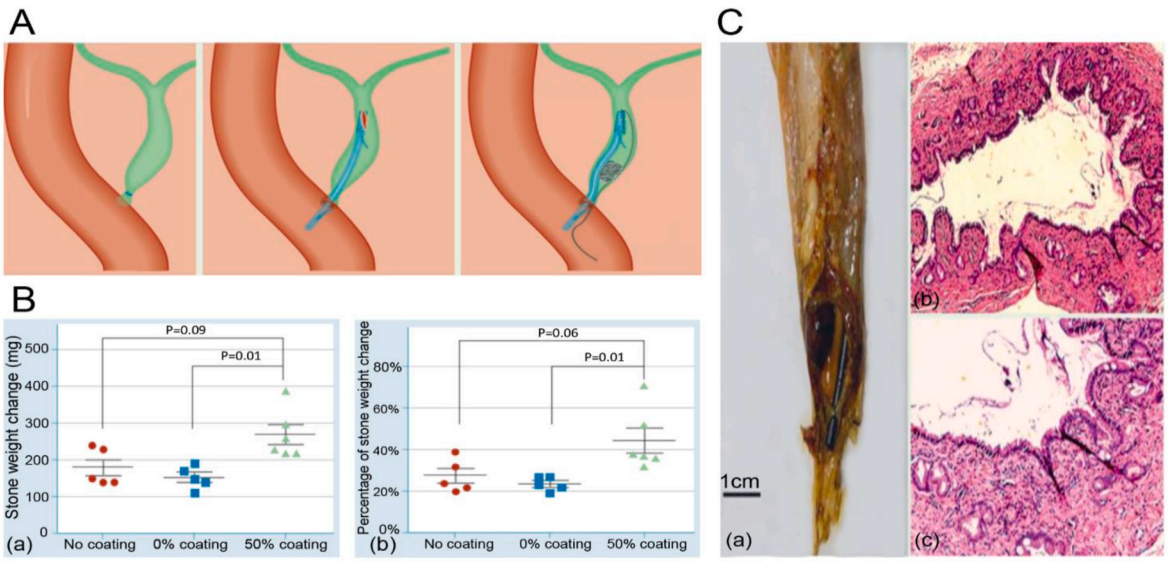

Fig. 7. Coated stents for stone dissolution in pigs [147]. **A:** Schematic illustration of the establishment of a CBD stone model and stent placement. (a) The distal part of the CBD was partially ligated to construct biliary stricture. (b) After longitudinal incision of the dilated CBD, the stone was placed in it. (c) A plastic stent was implanted. **B:** Stone weight changed in different stent groups. (a) Three groups of stone weight change (mg). Greater stone weight reduction was achieved in the 50 % coating group. (b) Similar results were obtained for the percentage change in stone weight. **C:** Histological findings in CBD that receiving a 50 % EDTA & SC-coated stent. (a) The CBD macroscopic appearance. (b) & (c) HE staining of CBD in the implanted portion of the stent, mucosa was smooth, but presence of mild inflammatory cell infiltration; × 100 (b), × 250 (c). HE: hematoxylin and eosin stain; CBD: common bile duct; EDTA: ethylenediaminetetraacetic acid; SC: sodium cholate.

Table 4
Stone-dissolving coatings.

Substrate	Coating			Evaluation			Ref
	Medicine	Material	Technique	In vitro	In vivo	Main result	
PS	E&S	E&S-PCL&PLA	Dip coating	Bile perfusion model	–	The coated PS effectively dissolved CBD stones.	[146]
PS	E&S	E&S-PCL&PLA	Dip coating	–	Pigs	The 50 % coated stent group had most stone weight loss than other groups.	[147]
Nitinol stent	E&S	E&S/PLCL	Electrospinning	PBS	–	Co-culturing with stones in PBS demonstrated its ability to dissolve stone.	[148]
FCSEMS	E&S	E&S-PCL	DCE	Still buffer, Flowing bile	Pigs	Stent III caused the most stone mass loss in vitro and showed good safety in pigs.	[149]
Metal stent	E&S	E&S-PLCL	Coaxial electrospinning Dip coating	Immersion in PBS	–	The electrospun coated stents exhibited stone-dissolving property, the fragments of stone became finer at day 7.	[150]

PS: plastic stent; E&S: ethylenediaminetetraacetic acid & sodium cholate; PCL: polycaprolactone; PLCL: poly-L-lactide-caprolactone; CBD: common bile duct; PLA: polylactide; FCSEMS: silicone covered self-expandable metal stent; PBS: phosphate-buffered saline; DCE: the coatings were prepared in different ways, Stent I, Stent II, and Stent III fabricated by dip coating, coaxial electrospinning, electrospinning combined with dip coating, respectively.

bacterial adhesion [185]. Enhancing the hydrophilicity of the material surface could prevent bacterial adhesion [186]. Hydromer, is a hydrophilic polymer, Hydromer-coated PU stent exhibited excellent resistance to bacteria in vitro.

[187]. However, in three subsequent clinical trials, these coated stents did not outperform uncoated PS

In treating malignant biliary strictures [188–190]. Kwon et al. [191] prepared a durable and uniform advanced hydrophilic coating inside of PS (with Hydak B-23K and Hydak T-060 as the base and top layers, respectively). Stenosis and biofilm formation were markedly lower in the coated group versus control group in vitro. However, the patency of coated and uncoated stents was not significantly different in porcine bile ducts after 8 weeks.

Hydrophobins are proteins produced by filamentous fungi, they self-assemble into amphiphilic membranes at hydrophilic and hydrophobic interfaces [192]. This protein film makes hydrophobic surfaces wettable, while hydrophilic surfaces become hydrophobic [193]. As stents usually possess a surface that is hydrophobic, the surface is rendered hydrophilic after being coated with hydrophobins. Weickert et al. [194] found that hydrophobins-coated PS reduced the material adhering to the stent surface. Combination with ampicillin/sulbactam or levofloxacin did not further reduce substances adhering to the stent surface, but coupling with high concentration of heparin reduced the adherent material. However, in a prospective randomized porcine study, there was no significant difference in patency in hydrophobins-coated stents or hydrophobins & Hep-coated stents compared to uncoated stents [195].

Conversely, material surface hydrophobicity is also an important factor in the adhesion of bacteria, which decreases with increasing hydrophobicity [196]. Seitz et al. [197] prepared inorganic-organic Sol--Gel hydrophobic coatings on the Teflon stents. In vitro tests revealed reduced sludge deposition on the coated surfaces than on the uncoated Teflon and hydrophobic Clearcoat coatings. However, they were not further validated in vivo, and other reports on hydrophobic biliary stents

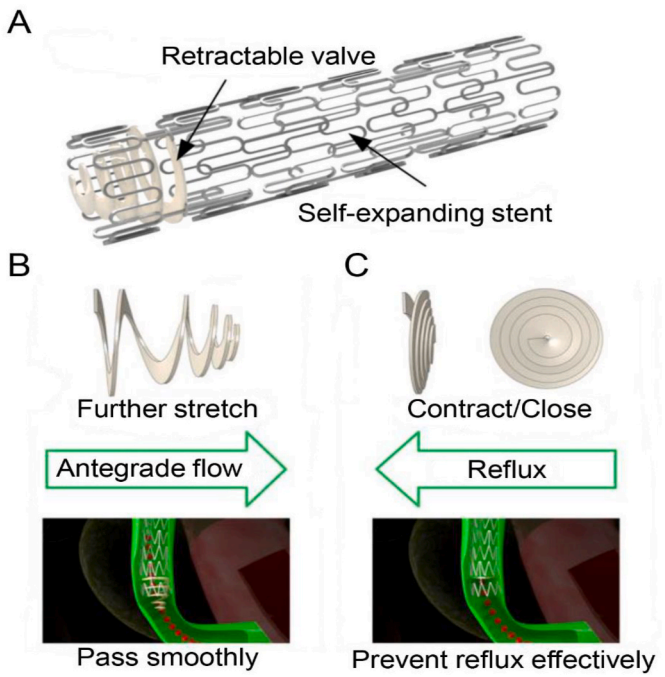

Fig. 8. Structure of a biliary stent with anti-reflux system [158]. **A:** Stent equipped with retractable valves. **B:** The state of the valve during the forward flow of bile, which passes smoothly through the valve. **C:** Valve status during reflux of duodenal contents, capable of preventing reflux effectively.

are lacking.

The use of hydrophilic or hydrophobic coatings to protect biliary stents from bacterial adhesion is possible, but the in vivo validation so far seems to refute this view. In fact, this is related to several

factors, such as the instability of the coating and the lack of superior hydrophobic or hydrophilic properties. Superhydrophobic(with static water contact angles >150°) and superhydrophilic surfaces(with static water contact angles <10°) with superior antimicrobial capabilities have received a widespread interest [198,199].On this basis, more stable, superhydrophobic or superhydrophilic coatings may be able to further reduce bacterial infection of the biliary stents.

4.3.4. Antibiotic-based coatings

Antibiotics such as ampicillin, sulbactam, cefotaxime and octenidine, etc., alone or in combination with other substances, have been used to prepare antibacterial coatings for biliary stents [194,200,201]. The coated stents showed significant antibacterial effects in vitro but did not prevent biofilm formation in vivo [200]. Failure to release antibiotics consistently and steadily, as well as the low concentration of antibiotics released, may contribute to surface biofilm formation on the stents. Furthermore, biofilms may be colonized by mixed microbial communities, including aerobic and anaerobic bacteria and fungi [202]. Therefore, these antibiotics may not completely prevent biofilm development. Notably, the development of antibiotic-based coatings requires caution, as antibiotic resistance has been reported in implant-associated pathogens [203]. Antimicrobial peptides (AMPs) are of great interest due to their low toxicity, spectra broad, and rapid antimicrobial behavior [204]. Compared to antibiotics, AMPs have a low chance of drug-resistance and can be coated on medical devices by adsorption, binding, and covalently conjugation [204]. In addition, some AMPs, such as ApoEdpL-W, show not only strong antibacterial but also antifungal activity (e.g., Candida albicans) [205,206]. As a result, AMPs-based coatings are expected to potentially show better antimicrobial and antibiofilm formation in biliary stents.

4.3.5. Other antibacterial or antibiofilm coatings

Chitosan [207–209], poly (2-methoxyethyl acrylate) and its derivative poly (3-methoxypropyl acrylate) [210,211], etc. have also been used for modification of biliary stents, either alone or in combination with other coatings. The effectiveness of these coatings is presented in Table 5. Other antibacterial strategies for biliary stents have been well summarized in this paper [153].

Among biliary stent coatings, antibacterial coatings are the most widely studied, but a few in vivo trials have shown that these coated stents were not effective in inhibiting stent occlusion. This may be related to the lack of long-term antibacterial activity of the coatings. Moreover, the antibacterial strategies of the above coatings are broadly classified as active (inactivating bacteria) and passive antibacterial (preventing bacteria from adhering) [212]. However, few researchers have combined these two strategies to achieve synergistic antibacterial effects. Currently, a combination of active and passive antibacterial coatings that display superior antibacterial capacity have been developed. The antibacterial agents (such as AgNPs [213], ZnO [214], Cu and its oxides [215,216], gold [214,217]) are incorporated into superhydrophobic or superhydrophilic coatings to realize a strong antibacterial effect. In addition, reducing surface roughness, controlling surface topography and stiffness, etc. will also improve antibacterial effect by reducing bacterial adhesion [185]. Therefore, improvements in these aspects of the coatings as well as the stents can be considered to reduce bacterial infection and biofilm formation.

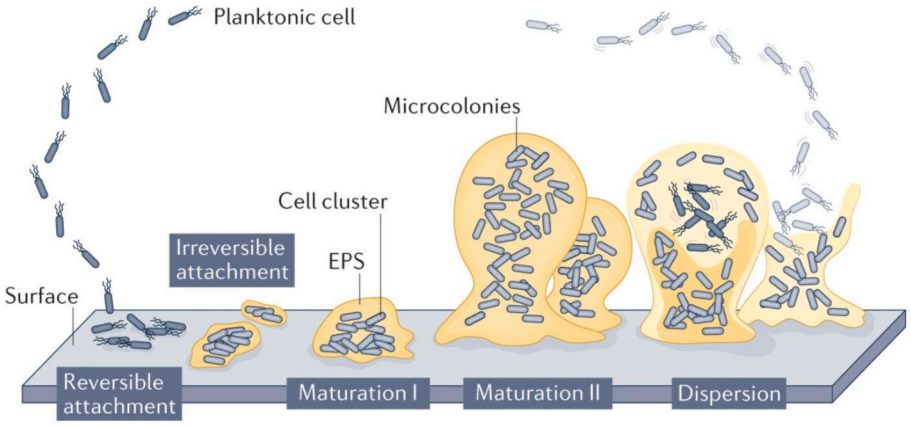

Fig. 9. Schematic diagram of biofilm formation [160]. Biofilm formation involves reversible and irreversible attachment, biofilm maturation, and eventually dispersion. EPS: extracellular polymeric substances.

Table 5
Antibacterial or antibiofilm coatings.

Substrate	Coating		Evaluation			Ref
	Material	Technique	In vitro	In vivo	Main result	
PS	AgNPs-Chitosan/ Hep	Layer by layer	*E. coli*	Pigs	The coated stents had a strong antibacterial capacity and significantly prolonged stent patency.	[163]
PU stent	AgNPs	Electrostatic adsorption	Immersion in bile	–	Biofilm formation on the surface of AgNPs-coated stents was significantly inhibited.	[164]
Teflon PS	AgNPs	Chemical oxidation–reduction	–	Dogs	The AgNPs-coated stent prevented sediment accumulation caused by obstructive jaundice.	[165]
PU stent	AgNPs/PU	Dip coating	–	Pigs	Coated stents were able to resist bacterial adhesion and reduce inflammation.	[166]
SEMS	AgNPs/PDA	Dip Coating	–	Rabbits	Stents with coatings prevented thermal damage, tissue proliferation and bacterial growth.	[169]
SEMS	AgNPs/PDA	Dip Coating	L929 293	Mice Rabbits	The coated stent was biocompatible and significantly inhibited stent-induced tissue proliferation and sludge formation.	[170]
PUPA	$HyalS_x$	–	EPKS	–	Reduced bacterial adhesion on coated surfaces compared to uncoated PUPA.	[182]
PE stent	Hep-PEI	Covalent immobilization	–	53 Patients	Heparin-coated stent was highly effective in preventing encrustation of stent.	[184]
PU stent	Hydromer	–	EKPE	–	A marked reduction in adherence to coated stents.	[187]
PU PE	Hydak B-23K/ Hydak T-060	Dip coating	Bile flow phantom model	Pigs	No significant difference in stent patency between coated and uncoated groups after 8 weeks.	[191]
PE stent	Hydrophobin*	Dip coating Covalent immobilization	Incubation in bile	–	Hydrophobin-coated PS reduced the adhesion on the stent. Coupling with antibiotics did not further reduce clogging, whereas coupling with high concentration of heparin reduced the adherent material.	[194]
SEMS	Hydrophobin Hydrophobin-Hep	Dip coating Covalent immobilization	–	Pigs	Clogging was not inhibited by coating with hydrophobin whether with or without Hep.	[195]
Teflon	Clearcoat IOSGC	Dip coating	Bile flow model	–	Sludge deposition was reduced on the IOSGC-coated Teflon as compared with the other.	[197]
CSEMS	Cefotaxime-PU/ PU	Dip coating	–	Dogs	Cefotaxime-coated stent did not prevent biofilm development.	[200]
PU	RO, RT ROC, RG	Dip coating	EEC	–	ROC-coated PU showed strong antimicrobial effect and high biocompatibility.	[201]
PE	Chitosan	–	CSPT	–	Adherence of *E. coli* to coated PE was higher than uncoated PE.	[207]
Glass Silicon	Chitosan Chitosan-κ-carrageenan	Covalent immobilization Layer by layer	BS385 BS11297	–	Coated surfaces were found to have reduced early bacterial deposition rates and the amount of bacterial attachment at a more advanced stage of the adhesion progression.	[208]
SS	Chitosan	Electrophoretic deposition	EE	–	The bacterial adhesion amount and colonization on the coated surface were significantly decreased.	[209]
CSEMS	PEMA PMC3A	Dip coating	Bile circulation	–	Protein adsorption/deformation and initial biliary sludge formation on coated stents were suppressed.	[210]
CSEMS	PEMA	Dip coating	–	Pigs	Coated stents with good biosafety showed mild fibrosis.	[211]

PU: Polyurethane; PS: plastic stent; SEMS: self-expandable metal stent; PE: polyethylene; PEI: polyethyleneimine; AgNPs: silver-nanoparticles; EPKS: *E. coli, Proteus* spp*, Klebsiella, Streptococcus.* $HyalS_x$: hyaluronic acid at a different stage of sulphation; PUPA: it was obtained by a poly(amido-amine) N_2LL interconnected with polyurethane chains using hexamethylene dyisocyanate as the cross-linking agent. EKPE: *E. coli, Klebsiella oxytoca, Proteus mirabilis, E. faecalis*.
PU: polyurethane; PE: polyethylene; SEMS: self-expandable metal stent; CSEMS: covered self-expandable metal stent; RO: resomer-octenidine; RT: resomer-triclosan; ROC: resomer-octenidine and citrate; RG: resomer-gentamicin; Hep: heparin; Hydrophobin*: three coatings, including hydrophobin with ampicillin & sulbactam, hydrophobin with levofloxacin and hydrophobin with Hep; IOSGC: inorganic-organic sol-gel-coating; PMEA: poly (2-methoxyethyl acrylate); PMC3A: poly (3-methoxypropylacrylate), EEC: *E. coli*, *E. faecalis*, *Candida albicans*; EE: *E. coli, Enterococcus*; CSPT: Closed stent perfusion testing.

4.4. Antiproliferative coating

Biliary trauma due to stenting or surgery, etc. cause fibroblasts to overpopulate, and the collagen they secrete can be deposited in large amounts, subsequently inducing biliary strictures. Common antiproliferative drugs such as PTX [218], steroids [219], and dexamethasone [220] have been used in antiproliferative coatings for biliary stents. Shi et al. [218] demonstrated that PTX-PLGA-coated PLLA stents suppressed the proliferation of myofibroblasts, the deposition of extracellular matrix, and reduced granulation tissue proliferation and glandular hyperplasia in the process of biliary-enteric anastomotic stoma healing in dogs. Jang et al. [219] showed that fibrous wall thickness in the steroid- PU-coated fully covered SEMS group decreased in the porcine benign biliary stricture model. Lee et al. [220] fabricated a biliary stent using PDX/PLLA filaments impregnated with dexamethasone, which has an antifibrotic action. This braided stent had an anti-fibrotic effect in vitro and in vivo, and disappeared after 16 weeks in the porcine bile duct, relieving benign biliary stricture. However, interest in biliary strictures caused by tissue hyperplasia remained limited. The few animals, the limited number of types of benign biliary strictures and the short observation period in these studies are all issues that need to be addressed in the future.

4.5. Corrosion-resistant coatings

Most of the biodegradable biliary stents mentioned above have not been able to provide long-term support within the bile ducts. Therefore, corrosion-resistant coatings are used in biliary stents to reduce premature loss of support from rapid stent degradation. As there are few reports on corrosion resistant coatings for polymer stents, the focus will be on Mg alloys. Zhang et al. [221] coated ZX20 stents with MgF_2-PCL using fluorinated treatment and dip coating methods. They showed that the coated stent could achieve compressive forces of 3.35–11.07 N and 11.09–24.08 N, and maintain the forces of 3.10–10.43 N and 3.11–9.37 N after 3 and 20 days of immersion in simulated bile, respectively. Guo et al. [222] reported that the MgF_2- poly (D, L-lactic acid) coating was effective in inhibiting the degradation rate of JDBM alloys in vitro and in vivo, but the support time was still less than 3 months. Coatings with enhanced corrosion resistance may be potential solution for prolonging the service life of Mg alloy stents in the bile ducts. For example, the

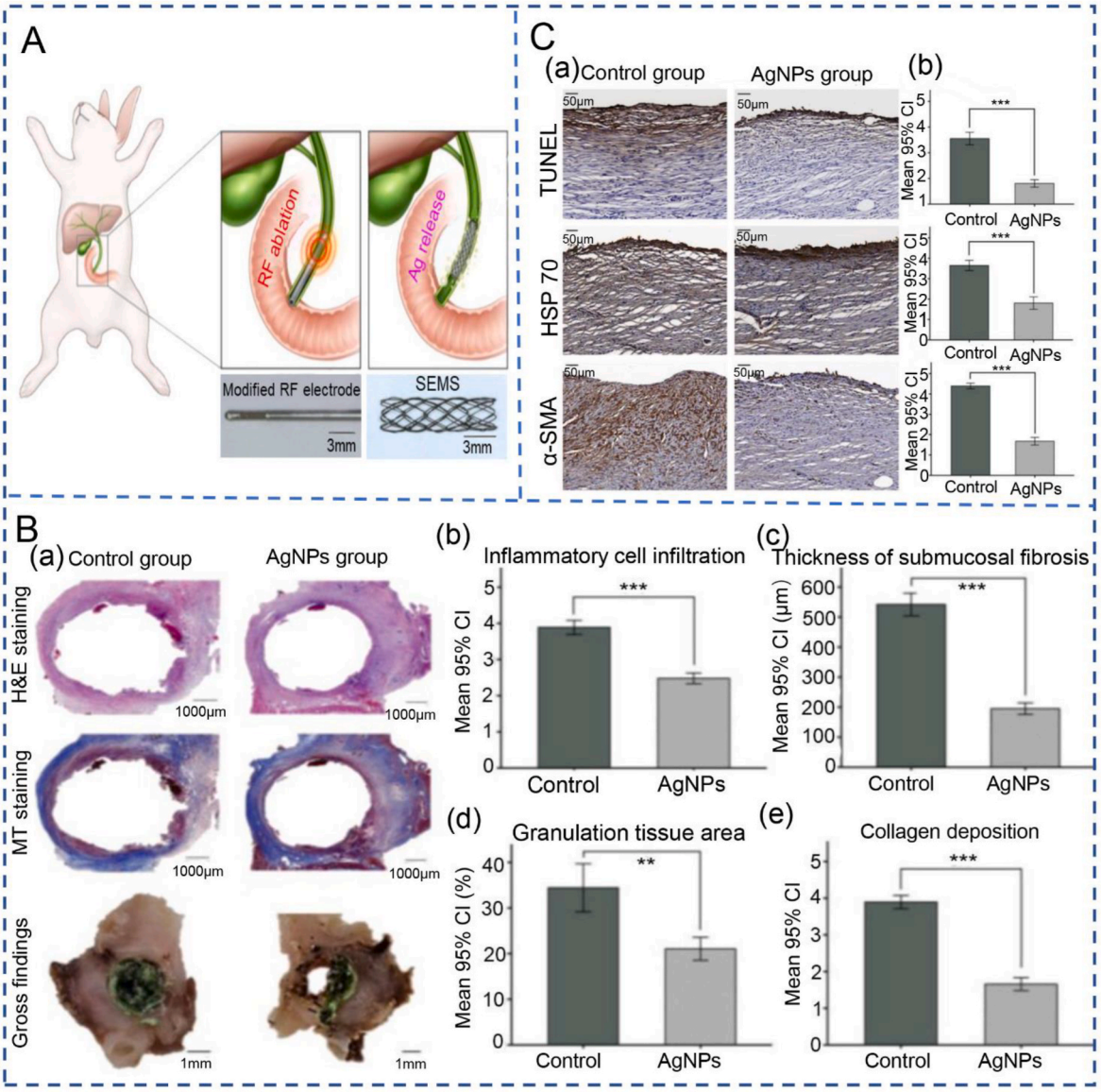

Fig. 10. Implantation of AgNPs-coated SEMS after RF ablation effectively blocked tissue hyperplasia and bacterial growth [169]. **A:** Schematic representation of SEMS coated with AgNPs placed immediately following RF ablation. **B:** Histological results and gross findings. (a) Representative pictures of the histological and gross results indicated that the extent of tissue hyperplasia in the AgNPs group was lower than in the control group. (b–e) Histological findings of the bile ducts in the stent-implanted portion of the control and AgNPs groups. **C:** The representative diagrams of the IHC staining and findings. (a) The photographs of TUNEL-, HSP 70-, and α-SMA-stained sections. (b) Results of quantitative analysis of histograms. AgNPs: silver nanoparticles; SEMS: self-expandable metal stent; RF: radiofrequency; PDA: polydopamine; TUNEL: terminal deoxynucleotidyl transferase-mediated dUTP nick and labeling; HSP 70: heat shock protein 70; α-SMA: α-smooth muscle actin. CI: confidence interval; $^{**}p < 0.01$; $^{***}p < 0.001$.

deposition of Ca-P coatings on AZ31B resulted in a corrosion current density that was two orders of magnitude lower than that of the substrate (bare:293 × 10^{-6} A cm^{-2}; coated:1.18 × 10^{-6} A cm^{-2}) [223]. Li et al. [224] fabricated Ca-deficient hydroxyapatite(HAp)/MgF_2 bilayer coatings on high-purity Mg, which showed increased resistance to degradation in SBF (bare: 331 μA/cm^2; coated: 2.24 μA/cm^2), Fig. 11A and B. In addition, the bilayer coating enhanced the proliferation of MG63 cells compared to the monolayer HAp and MgF_2 coatings, Fig. 11C. Nowadays, strategies to enhance the corrosion resistance of Mg and its alloys have been more widely developed and applied to implantable devices [225–227]. These excellent corrosion-resistant coating strategies may also be suitable for biliary stents.

In conclusion, considerable effort has been made to develop functional coatings for biliary stents, but improvements are still needed in the future. However, most of these were preliminary in vitro experiments, only a small fraction was evaluated in vivo and the results were not promising. The poor in vivo results may be explained by the following reasons: 1) Stability of the coating: owing to the biodegradability of the material, the corrosiveness of the physiological environment, and the need for deformation such as gripping and expansion during stent implantation, this will inevitably damage the stent coating, leading to micro warpage or microcracks [228,229]. Corrosion will initiate at the point of damage to the coating, leading to failure of the implantation operation or premature failure of the stent during its lifetime [228]. To address these issues, intelligent coatings with self-healing properties, inspired by the healing process of natural organisms, have been proposed and developed for Mg alloy [229]. In general, a self-healing coating developed for corrosion protection consists of a barrier coating and incorporated corrosion inhibitors, and the loaded corrosion inhibitors can react with the resulting Mg^{2+} or OH^- to form

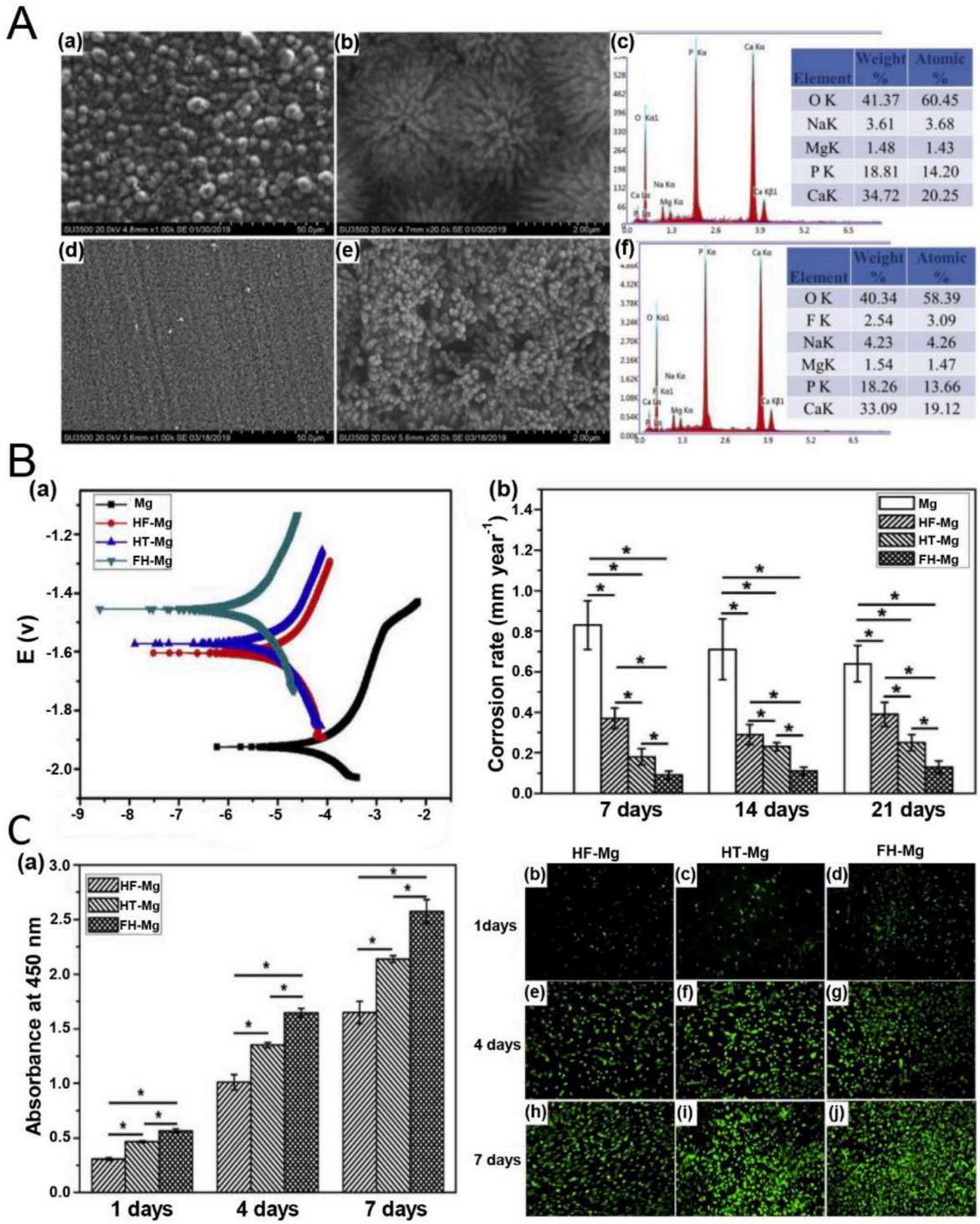

Fig. 11. The HAp/MgF double-layer coating on biodegradable high-purity Mg [224]. **A:** Surface morphologies and element components of HT-Mg **(a–c)** and FH-Mg **(d–f)**. **B:** Polarization curves (a) and (b) corrosion rate for Mg, HF-Mg, HT-Mg, and FH-Mg after immersion test in SBF solution for 7, 14, and 21 days. **C:** Cytocompatibility of HF-Mg, HT-Mg, and FH-Mg. (a) MG63 cells proliferation after 1-, 4-, and 7-days incubation. Live-dead staining of MG63 cells cultured on the surface of HF-Mg (b, e, h), HT-Mg (c, f, i), and FH-Mg (d, g, j) at day 1, 4, and 7. *$p < 0.05$.

relatively stable precipitates and repair the defect as the barrier coating is damaged and local corrosion occurs [230]. Recently, Guan et al. [228] fabricated sol-gel coatings incorporating various corrosion inhibitors on the surface of ZE21B alloy. Among them, paeonol condensation tyrosine exhibited excellent corrosion resistance, notable self-healing ability, and also showed enhanced proliferation of HUVEC cells. Therefore, such self-healing coatings may also be used to develop stable, long-term drug-releasing coatings for biliary stents. 2) Inadequate in vitro evaluation: biofilm formation on the stent was caused by a combination of proteins and multi-microbial communities, and the use of a single or a few bacterial species was insufficient. More representative strains should be included in future antibacterial assessments to test for prolonged antibacterial and antibiofilm formation capabilities 3) Single functional coatings: stenosis or blockage of the stent was often caused by

multiple factors. It is not effective in preventing stent or blockage with a single functional coating. Hence, the development of multi-functional coatings is necessary.

5. Tissue engineering & 3D-printed stents

5.1. Tissue engineering stents

Advanced tissue engineering techniques and biomaterials have been employed for organ or tissue regeneration. Autologous tissues, collagen, cells (e.g., mesenchymal stem cells, cholangiocytes), and acellular matrix are adapted to repair and reconstruct the bile duct. Heistermann et al. [231] implanted an autologous vein graft that was splinted by PLA stent into pig for CBD reconstruction. After 4 months, bile duct reconstruction was complete, the stents were fully degraded, and the vein graft had been relined with biliary epithelium. In another study, a new stent was manufactured from poly [sebacic acid-co-(1, 3-propanediol)-co-(1,2-propanediol)]. Around the stent and both ends

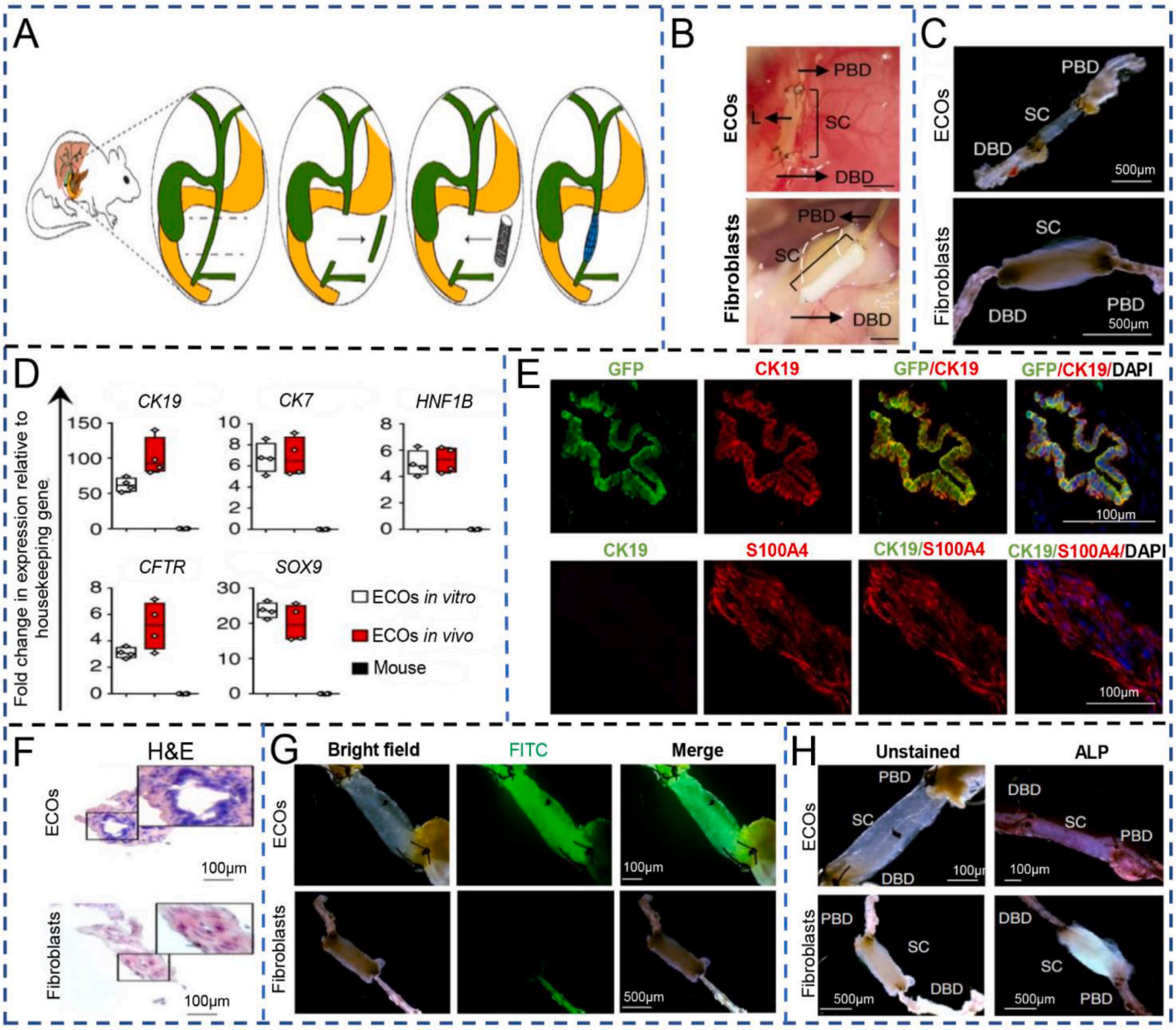

Fig. 12. Replacement of bile duct with ECO-populated densified collagen tubes [242]. **A:** Schematic illustration of the procedure for the replacement of the bile duct. **B:** Postmortem pictures of mice receiving a collagen tube populated with ECOs (ECOs) compared to a FPT (fibroblasts). Yellow pigmentation of EPT due to bile flow. Luminal obstruction causing bile leakage (yellow peritoneal pigmentation, white dashed line) is indicated by the white color of the fibroblast-populated conduit and the expanded, and bile-laden (yellow color) PBD, (scale bars, 500 μm). **C:** Pictures of a thin-walled native bile duct-like construct from a mouse that received an EPT compared to a thick construct with no discernible lumen generated from a mouse that received the FPT. **D:** qRT-PCR analyses demonstrating bile duct marker expression by ECOs from ECO-populated transplanted tubes (ECOs in vivo) versus cultivated ECOs (ECOs in vitro) and bile duct tissue from mice as the negative control.; n = 4 tubes. Box, IQR; center line, median; whiskers, range (minimum to maximum). The values are relative to the expression of HMBS. **E:** IF analyses revealing lumen lining of GFP + CK19+ epithelium in the EPC compared to lumen obliteration by fibroblasts in the FPC. **F:** H&E staining showing the existence of biliary epithelium and patent ductal lumen in EPT but not in FPC. **G:** Cholangiography with FITC demonstrating luminal patency in EPT as opposed to luminal occlusion in FPC. H: The activity of ALP is observed exclusively in EPT, but not in FPC. ECOs: extrahepatic cholangiocyte organoids; PBD: proximal bile duct. SC: collagen tubular scaffold; DBD: distal bile duct. HMBS: housekeeping gene hydroxymethylbilane synthase; EPC: ECO-populated construct; EPT: ECO-populated tube; FPC: fibroblast populated construct; FPT: fibroblast-populated tube; ALP: alkaline phosphatase.

of the CBD, the vascularized greater omentum was placed. After 3 months of stent implantation, stent disappeared completely and the porcine CBD was well repaired without serious complications [232].

Collagen with good biocompatibility, biodegradability, cell activities, and mechanical properties, is widely used in biomedical applications, such as wound healing and tissue engineering [233]. Montalvo et al. [234] prepared the stents using collagen and deposited the PCL membrane on the stent surface to prevent bile leakage and to waterproof. In a 6-month observation, no stenosis or obstruction occurred in porcine CBD, indicating that the stent could be used as a replacement for bile duct in patients with cancer or biliary injury.

Mesenchymal stem cells (MSCs) possess multipotency property and exhibit great potential in immunomodulation and tissue regeneration [235]. Zong et al. [236] inoculated human bone marrow-derived MSCs onto the PCL/PLGA bilayer stents. After 6 months, the designed stents were more advantageous in repairing damaged bile ducts without stenosis and cholestasis. Zhang et al. [237] demonstrated that PS wrapped in MSCs-seeded mesh was safely applied to biliary anastomoses without complications. They further found that MSC-coated PDX stents reduced peri-biliary fibrosis and significantly increased neoangiogenesis in a porcine choledochojejunostomy model [238]. Yan et al. [239] fabricated bilayer tubular stents for bile duct regeneration, with PLGA and gelatin methacrylate (GelMA)/poly (ethylene glycol) diacrylate as inner and outer layers, respectively. Furthermore, cholangiocyte-like cells derived from induced MSCs were inoculated into the outer layer. After 12 weeks, the stents with induced MSCs facilitated bile duct repair and promoted regeneration of the biliary epithelium compared to the PLGA monolayer stent.

Biliary complications are the primary reason for liver transplantation failure [240]. Treatment options remain limited due to a lack of available healthy donor tissue from which to rebuild and substitute the diseased bile duct [241]. Therefore, Sampaziotis et al. [242] integrated in vitro expansion of cholangiocytes with tissue-engineered stents to address this limitation. They propagated human cholangiocytes in vitro and formed extrahepatic cholangiocyte organoids (ECOs). When ECOs was implanted on the biodegradable stents, tissue-like structures were formed that preserved the characteristics of the bile ducts. The bioengineered tissue was able to repair the biliary epithelium and rebuild the gallbladder wall after implantation in mice. In addition, bioengineered bile ducts can serve as a substitute for native CBD, and no cholestasis or obstruction occurred, Fig. 12.

Acellular matrix materials have been favored in tissue engineering because of their excellent biocompatibility and degradability, which promote cell growth and tissue repair [243–245]. Jiang et al. [241] constructed artificial bile ducts for the regeneration of porcine bile duct defects using ureteral acellular matrix and biodegradable polyurethane. After implantation, the presence of biliary epithelial cells was observed on day 70 and a contiguous biliary epithelial layer was formed at day 100.

These tissue-engineered stents are promising, but the relatively cumbersome and time-consuming preparation steps may limit their widespread application. Effective implantation of cells or tissues and maintaining their activity are also current challenges.

5.2. 3D-printed stents

Stents manufactured with traditional methods have a very narrow range of sizes and lack customization. 3D printing technology can be used to rapidly customize stents [246]. Park et al. [247] prepared thin-Walled Free-Form PVA stents (with PCL coating) using 3D printing. No abnormal histological changes were detected 3 days after implantation of these stents in rabbits. However, the study lacked long-term observation to evaluate its biliary reconstruction ability. Kim et al. [248] also showed that 3 months after implantation of 3D-printed PCL stents into pigs, the stents fragmented and.

The bile ducts exhibited only mild inflammation and fibrosis. This suggested that the stents had the potential to prevent postoperative biliary strictures. Li et al. [249] fabricated the GelMA hydrogel coating on the surface of 3D-printed PCL stents, which not only protected and supported the stents but also improved the biocompatibility of the stents. In addition, ultra-small superparamagnetic iron oxide nanoparticles were dispersed in GelMA to serve as a contrast agent. However, they did not use relevant cell lines and animals to validate their biliary repair ability.

The combination of tissue engineering and 3D printing technology could produce customized more bio-biliary stents [4]. In a proof-of-concept study, Boyer et al. [250] injected collagen, human placental MSCs, and cholangiocytes into 3D-printed crosslinked PVA stents. It was anticipated that the design elements used in the stent would allow for proper placement of the stent, protect the stem cell matrix of the stent from bile components, and inhibit biofilm formation. Xiang et al. [251] designed a bilayer stent consisting of PLGA and GelMA. The inner layer of PLGA was strong enough to support

bile duct constriction, and the outer layer of GelMA was biocompatible to provide a favorable environment for cells survival. In addition, the IKVAV laminin peptide and ultra-small superparamagnetic iron oxide were used to regulate stents cell adhesion and magnetic resonance imaging detection, respectively. After 14 days of implantation in pigs, the bilayer stents promoted enhance the expression of cytokeratin 19 and bile duct regeneration.

Overall, the initial results achieved with tissue engineering and 3D-printed stents were satisfactory, but there are still issues that need to be surmounted. One of the main problems is the resolution of the printer, which limits the fabrication of thinner stent struts, followed by strut smoothness and homogeneity, and stent sterilization [246].

6. Future perspectives

Current biodegradable biliary stents, surface modification, tissue engineering & 3D-printed stents overcome many of the drawbacks of conventional stents, such as short patency and the necessity of additional surgical interventions. However, there is still considerable scope for the enhancement of these stents and technologies to meet clinical requirements. Based on the literature, we propose the following four possible future directions for biliary stents: 1) pro-epithelialization coatings; 2) multifunctional coated stents; 3) biodegradable shape memory stents; 4) 4D bioprinting.

6.1. Pro-epithelialization coatings

Bacteria were absent from natural bile duct walls and gallbladder walls [252]. As a consequence of stent implantation, epithelial cells are inevitably damaged and stripped. The stents were at least partially embedded in the bile ducts through inflammation and foreign body reactions. Furthermore, the stent surface was covered by a layer of fibrogranubomatous tissue rather than the epithelial layer formed by natural epithelial cells. In segments without bile duct epithelium where the stent was placed, the stent surface may be susceptible to bacterial colonization, which could induce the process of sludge formation. The exfoliation of superficial fibroblastic cells and necrotic tumor cells on the stent may also lead to sludge formation [253]. Therefore, the development of functional coatings that promote the epithelialization of biliary stents is of great research interest. Because these coatings promote the repair of damaged biliary epithelium, are expected to reduce biofilm formation and tissue hyperplasia. Presence of biliary stem/-progenitor cells in peribiliary glands existing in extrahepatic bile ducts. These glands proliferate when the bile ducts are damaged and produce new choanocytes to rebuild the bile duct lining [254]. Accordingly, the loading of these cells as well as the creation of an environment conducive to the adhesion of renewed choanocytes to the stent is anticipated to promote repair of the damaged bile ducts. Moreover, IL-33 significantly promoted the proliferation and sustained growth of mice

cholangiocytes. An increase in the number of type 2 innate lymphoid cells (ILC2s) mediated the IL-33-dependent proliferative response. High levels of IL-13 released by ILC2s promoted cholangiocyte hyperplasia. Biliary epithelial repair promoted by induction of IL-33/ILC2/IL-13 pathway in murine bile duct injury model [255]. Thus, loaded stents with IL-33 or IL-13, as well as activators of the IL-33/ILC2/IL-13 pathway, may have the potential to promote repair of damaged bile ducts remodel strictures. In addition, the activation of the IL-33/ILC2/IL-13 circuit in mice with constitutive AKT and YAP activation in the biliary also led to the emergence of cholangiocarcinoma with liver metastases [255]. Therefore, inhibitors that block this circuit may also serve for the preparation of antitumor coatings. Other biomolecules such as miR-124, miR-200, and IL-6 are closely related to the proliferation of cholangiocytes and can be explored as pro-epithelialization coatings [256].

6.2. Multifunctional coated stents

In-stent restenosis is caused by multiple factors, and it may be difficult to inhibit stenosis using a single functional coating. Stents loaded with multifunctional coatings with synergistic anti-stenosis effects may be effective in prolonging stent patency. Currently, there are few reports about multifunctional coatings for biliary stents. Tian et al. [257] designed novel tri-layer films for biliary stents with PTX layer (PLA loads PTX), isolation layer (drug-free PLA), and OFLX layer (PLA loads ofloxacin) as inner, middle, and outer layers, respectively. The

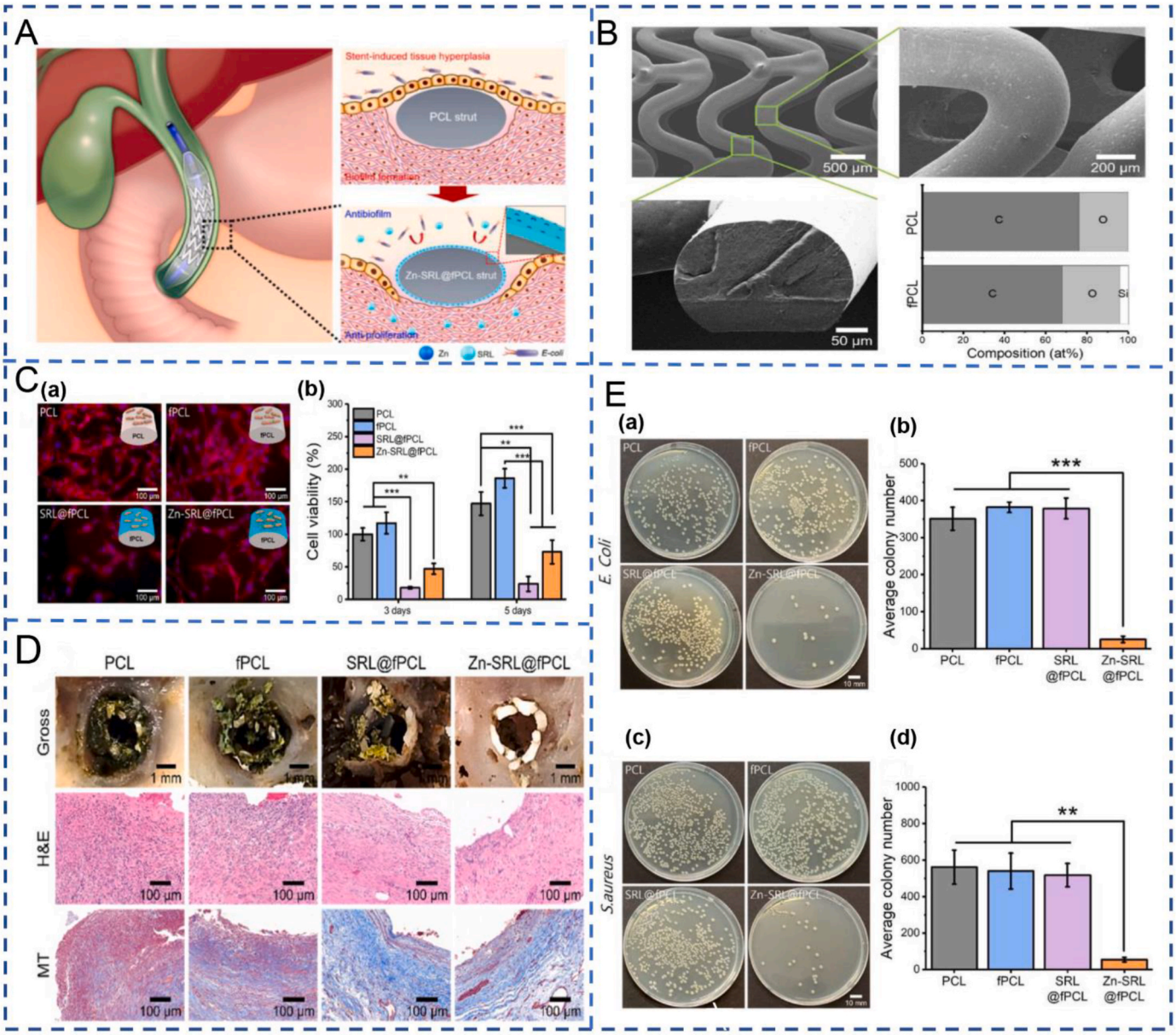

Fig. 13. 3D-printed biliary stents for anti-hyperplasia and antibiofilm formation. **A:** The elliptical strut promotes bile flow to reduce precipitate formation, and the hydrophilic surface and antibacterial Zn ions inhibit bacterial adhesion and biofilm formation. **B:** Representative FE-SEM images of 3D-printed fPCL stent (a) and chemical compositions of 3D-printed fPCL and pristine PCL stents (b). **C:** Anti-fibroblast proliferative activity. **(a):** CLSM micrographs of fibroblasts on different specimens after 24 h of culturing and (b) proliferation of fibroblasts on different specimens after 3 and 5 d of culturing. D: Macroscopic and microscopic images 4 weeks after stent placement in rabbit common bile duct. (b) Histological results of 3D-printed PCL, fPCL, SRL@fPCL, and Zn-SRL@fPCL stent groups in the stented bile duct. **E:** Evaluation of bactericidal activity. (a) Optical pictures and (b) mean colony counts of *E. coli*. (c) Optical pictures and (d) average colony counts of *S. aureus*. *p < 0.05, **p < 0.01, ***p < 0.005, and ****p < 0.001.

adhesion of *E. coli* and *S. aureus*, biofilm formation, and proliferation of the human cholangiocarcinoma cells were effectively inhibited by this coating in vitro. Similarly, Rezk et al. [258] prepared a triple-layer membrane, and the bottom, middle and top layers were AgNPs-PU, PTX-PU and PCL, respectively. However, they only verified the strong antibacterial effect of the coating. Li et al. [259] constructed the nano-engineered surface layer on the sirolimus-coated functionalized PCL stents using Zn ion sputtering-based plasma immersion ion implantation treatment, Fig. 13A and B. The resulting functionalized surface significantly reduced bacterial responses and fibroblast proliferation in vitro, Fig. 13C and E. They also showed that stents with functionalized surface significantly inhibited granulation tissue and biofilm formation with good stent patency in rabbit CBD, Fig. 13D. The advantages of multifunctional coatings have been initially demonstrated, but the superiority of these multifunctional coatings over monofunctional coatings needs to be verified by additional in vivo test and long-term observation. In addition, coatings that simultaneously increase the corrosion resistance of the material and are antibacterial or antitumor, antibacterial and antiproliferative, or triple-function coatings (antibacterial, antitumor, and Corrosion-resistant) are multifunctional coatings that have yet to be developed [7]. These coatings are theorized to exert a synergistic effect in preventing in-stent restenosis, thereby enabling a longer patency period in line with clinical needs [257,259].

Furthermore, there is a need to reduce the side effects of coating drugs. Stent-loaded drugs (e.g., antitumor drugs, AgNPs) are usually not specific and have significant side effects on surrounding tissues or cells

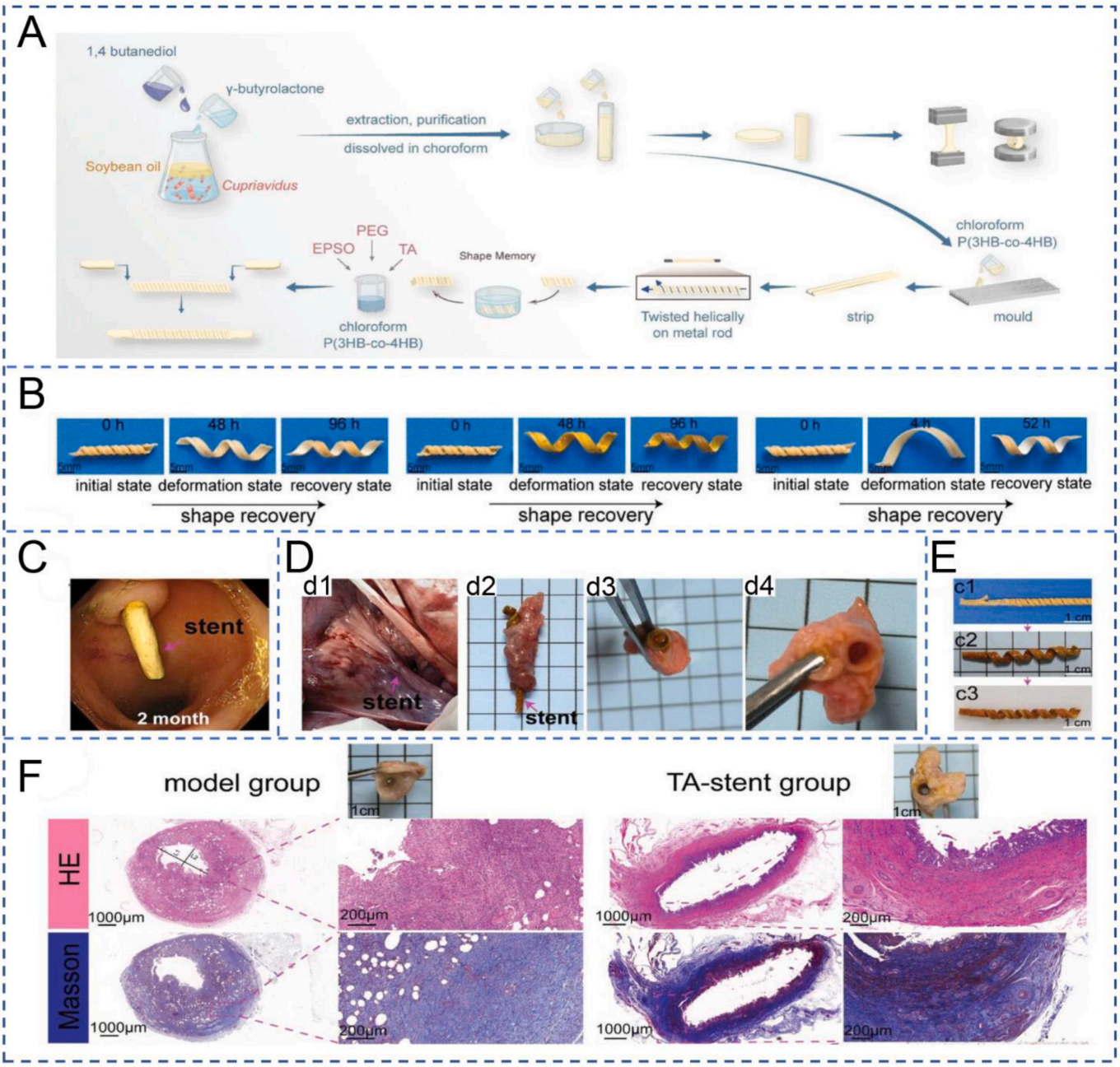

Fig. 14. 3D printing-based biodegradable shape memory biliary stents [61]. **A:** The stent manufacturing process. **B:** Shape recovery of the P(3HB-co-4HB) stent in 37 °C PBS, bile, and alcohol at different time points. **C:** Stent morphology after insertion of 2 months (under endoscope). **D:** The position of the stent and common bile duct. **E:** Shape memory characteristics of the stent at different times. c1) The initial stent. c2) Fresh stent just removed from bile duct. c3) The dried stent removed from bile duct. **F:** Histologic staining of bile duct. TA: triamcinolone acetonide; PEG: polyethylene glycol; EPSO: ethiodized poppy seed oil.

[260–262]. Damage to bile duct tissue is unavoidable with stent coatings that attach to the bile duct wall. Asymmetric coatings with different functions on the luminal surface of the stent and the stent surface in contact with the bile ducts could effectively mitigate this shortcoming. Antibacterial coatings are formed on the luminal surface of the stent, while antitumor, antiproliferative.

or pro-epithelialization coatings are applied to the stent surface against the wall of the bile ducts. Inspired by asymmetric coatings for vascular stents, these asymmetric functional coatings can reduce

Drug side effects, prevent biofilm formation on the stent surface, tissue hyperplasia or promote biliary epithelium repair [260].

6.3. Biodegradable shape memory stents

Stents with shape memory could provide real-time adjustment of the correction/support and also significantly increase healing efficiencies associated with implants and devices [263]. However, SEMS are non-degradable, so the development of biodegradable shape memory stents is one of the future research directions. Biodegradable shape memory materials including biodegradable shape memory polymers (BSMP) and biodegradable shape memory alloys (BSMA). PCL, PLA and lactic acid-based copolymers are the main types of BSMP. BSMP are usually less dense, easy to process, lightweight and cheaper than BSMA [264]. Recently, Wang et al. [61] reported a novel biodegradable helicoidal stent made of biosynthesized P(3HB-co-4HB), that exhibited shape memory in various solvents, Fig.

14A-B. The stent was able to automatically expand in the porcine narrowed bile ducts. After implantation, the stent patency was good, the stent loaded triamcinolone acetonide effectively inhibited tissue proliferation Fig. 14C–F. Nevertheless, it was slow to recover its shape and did not rapidly expand the narrowed bile ducts, which may reduce its potential for applications.

BSMA mainly consists of Mg-based, Fe-based, and Cu-based alloys [263]. The addition of the element scandium (Sc, 20 at%) resulted in Mg alloys with shape memory properties [265]. Subsequently, $MgSc_xX_y$ ternary alloys [x = 13–30 at%, y = 0.001–9 at%, X = Zn, Li (lithium), Al (aluminum), Y (yttrium), Ag (silver), In (indium), Sn (stannum), and Bi (bismuth)] were considered as Mg-based SMA [263]. The mechanical properties and corrosion resistance of the Mg-Sc alloys were significantly enhanced, and showed excellent biocompatibility. For example, Mg-30 wt% Sc SMA (with ultimate compressive strength of 603 ± 39 MPa and compressive strain of 31 ± 3 %) degraded in vivo at a rate of only 0.06 mm $year^{-1}$, and the implant retained its mechanical integrity even after 24 weeks of implantation in rat femurs [266]. Despite the low long-term corrosion rate, the rapid corrosion rate of Mg-Sc SMA during the early corrosion process or before the formation of sufficient surface passivation further requires mitigation to prevent both undesirable gas cavities and swelling induced by excessive H_2 evolution [263]. Moreover, $MgSc_xX_y$ ternary alloys need to be explored for their potential medical applications. The biocompatibility and mechanical properties of Fe-based BSMA are well established, but their slow degradation rate still needs to be overcome. Alloying, composite design, surface modification, phase manipulation, defect introduction, fabrication of porous structure are all effective solutions to enhance the corrosion rate of Fe-based SMA [263]. Cu-based BSMA mainly include Cu-Zn, Cu-Al binary alloys, and Cu-Zn-Al, Cu-Al-Ni ternary alloys [267]. Cu-based BSMA are easy to fabricate and have good shape recovery, but high transition temperature and brittleness, low thermal stability, low mechanical strength, and poor biocompatibility limit their medical applications [267,268]. There is still a necessity to optimize the elemental ratios of the alloys for improving their mechanical properties, flexibility, and lowering the transition temperature. In addition, the use of copper chelators to avoid sudden and large releases of copper ions is one way to improve the biocompatibility of copper-based SMAs [269,270]. Biodegradable shape memory materials have shown great advantages in medical application. The issues that cannot be ignored include the transition temperature, shape recovery speed, degradation rate, and biocompatibility. These properties need to be optimized in the future to match the physiological environment of the bile ducts.

6.4. 4D bioprinting

3D bioprinting technology is capable of creating complex 3D functional tissue structures. However, this approach has one major drawback: it only considers the initial state of the object, which

Is assumed to be static and inanimate [271]. 4D bioprinting, which combines the concept of time with three-dimensional 3D bioprinting technology as the fourth dimension [272]. The objective of 4D bioprinting is to generate more sophisticated structures that exhibit the capacity to modify their.

Properties in response to internal or external triggers (e.g., temperature, electric or magnetic fields, humidity, light, ions, pH, enzymes, antigens, glucose), with the aim of repairing, regenerating, or replacing diseased or damaged cellular, tissue, or even organ tissue [273]. Consequently, 4D bioprinting provides a novel pathway for the advancement of biodegradable shape memory biliary stents [274]. 4D bioprinting can also be used for the development of advanced, dynamic and controlled stent-based drug delivery systems. These smart biomaterial-based stents tailor drug release or morphology to inhibit the growth of tumor cells or bacterial in response to specific environmental stimuli (e.g., locally ROS and elevated pH in the tumor environment, lipopolysaccharides produced.

by bacteria, etc.) [275,276], Fig. 15. In addition, 4D bioprinting enables the creation of artificial tissues that are more structurally and functionally analogous to native tissues and have the ability to dynamically and intelligently respond to environmental changes and regulate cellular behavior [273].

7. Summary

Non-degradability and susceptibility to in-stent restenosis are the main disadvantages of conventional stents, which require surgical removal and prompt replacement. The developments in materials and surface modification technologies have effectively mitigated these deficiencies. Although biodegradable biliary stents avoid additional surgical removal, there are several areas that require further enhancement, including the insufficient support time, poor mechanical properties, and biocompatibility. Surface modification of the stent could prolong the stent patency, but there is still room for improvement in terms of stability and efficacy. Tissue engineering and 3D-printed stents enable rapid repair and reconstruction of the bile duct, maintaining the high activity of implanted cells, tissues or other biologically active materials and improving the efficiency of implantation are issues worth exploring. In the future, advanced surface modifications, biodegradable shape memory materials, and 4D bioprinting technologies will significantly accelerate the development of the ideal biliary stent.

Conflicts of interest

All the authors read and reviewed the manuscript and agreed to its publication.

Ethics approval and consent to participate

This work does not involve the use of human subjects or animal experiments.

CRediT authorship contribution statement

Yuechuan Li: Writing – original draft, Visualization, Methodology, Formal analysis, Data curation. **Kunshan Yuan:** Writing – review & editing, Visualization, Investigation, Formal analysis. **Chengchen**

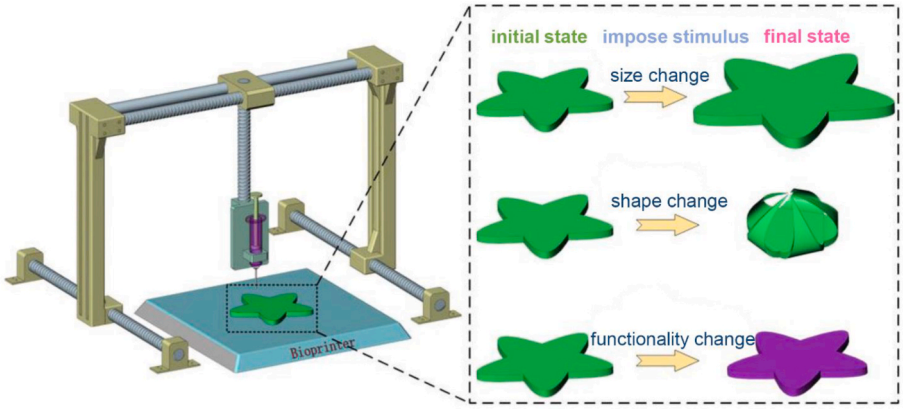

Fig. 15. Schematic representation of 4D bioprinting [275]. The printed bioconstruct can alter its size, shape or functionality in response to external stimuli.

Deng: Writing – review & editing. **Hui Tang:** Investigation. **Jinxuan Wang:** Formal analysis. **Xiaozhen Dai:** Resources. **Bing Zhang:** Investigation. **Ziru Sun:** Formal analysis. **Guiying Ren:** Visualization. **Haijun Zhang:** Writing – review & editing, Supervision, Conceptualization. **Guixue Wang:** Supervision, Funding acquisition, Conceptualization.

Declaration of competing interest

All authors declare that there are no competing interests.

Acknowledgments

This work was supported by grants from the Fundamental Research Funds for the Central Universities (No. 2024CDJCGJ-016) and National Natural Science Foundation of China (No. 82270535), the Science and Technology Innovation Project of Jinfeng Laboratory, Chongqing, China (jfkyjf202203001) and China Postdoctoral Science Foundation (2023MD734198). We are also thankful for the First Batch of Key Disciplines on Public Health in Chongqing and the Public Experiment Centre of State Bio Industrial Base (Chongqing), China.

References

[1] S. Liu, M. Yi, J. Qin, et al., The increasing incidence and high body mass index-related burden of gallbladder and biliary diseases-A results from global burden of disease study 2019, Front. Med. 9 (2022).
[2] B.J. Elmunzer, J.L. Maranki, V. Gómez, et al., A CG clinical guideline: diagnosis and management of biliary strictures, Am. J. Gastroenterol. 118 (3) (2023) 405–426.
[3] G. Song, H.Q. Zhao, Q. Liu, et al., A review on biodegradable biliary stents: materials and future trends, Bioact. Mater. 17 (2022) 488–495.
[4] S. Choudhury, S. Asthana, S. Homer-Vanniasinkam, et al., Emerging trends in biliary stents: a materials and manufacturing perspective, Biomater. Sci. 10 (2022).
[5] J.-H. Chen, H.-P. Wang, Endoscopic retrograde cholangiopancreatography training and education, Dig. Endosc. 36 (1) (2024) 74–85.
[6] R. Lam, T. Muniraj, Fully covered metal biliary stents: a review of the literature, World J. Gastroenterol. 27 (38) (2021) 6357–6373.
[7] K. Yang, W. Sun, L. Cui, et al., Advances in functional coatings on biliary stents, Regen. Biomater. 11 (2024) rbae001.
[8] B. Dinescu, T. Voiosu, A. Bengus, et al., The Perfect Biliary Plastic Stent: the Search Goes on, Ann. Gastroenterol., 2023.
[9] S. Han, J.V. Obando, A. Bhatt, et al., Biliary and pancreatic stents, iGIE 2 (2) (2023) 240–253.
[10] A. Blanco-Míguez, S. Carloni, C. Cardenas, et al., Microbial composition associated with biliary stents in patients undergoing pancreatic resection for cancer, npj Biofilms and Microbiomes 10 (1) (2024) 35.
[11] F. Kamal, M.A. Khan, W. Lee-Smith, et al., Metal versus plastic stents in the management of benign biliary strictures: systematic review and meta-analysis of randomized controlled trials, Eur. J. Gastroenterol. Hepatol. 34 (5) (2022) 478–487.
[12] A. Yamabe, A. Irisawa, Y. Kunogi, et al., Development of biliary stent applying the antibacterial activity of silver: a literature review, Bio-Med, Mater. Eng. 32 (2) (2021) 63–71.
[13] M. Colombo, E. Forcignanò, L. Da Rio, et al., Endoscopic management of benign biliary strictures: looking for the best stent to place, World J. Clin. Cases 11 (31) (2023) 7521–7529.
[14] A. Kubesch, F. Görnert, N. Filmann, et al., Impact of a shorter replacement interval of plastic stents on premature stent exchange rate in benign and malignant biliary strictures, J. Gastroenterol. Hepatol. 37 (6) (2022) 1076–1082.
[15] V.D. Yagnik, A. Patel, G.M. Mannari, et al., Migration of biliary stent into the gallbladder: a surprising intraoperative finding, J. Minimal Access Surg. 18 (1) (2022) 151–153.
[16] B.H. Cha, M.J. Jang, S.H. Lee, Survival benefit of intraductal radiofrequency ablation for malignant biliary obstruction: a systematic review with meta-analysis, Clin. Endosc. 54 (1) (2021) 100–106.
[17] T. Mukai, K. Iwata, T. Iwashita, et al., Comparison of covered self-expandable metallic stents with 12-mm and 10-mm diameters for unresectable malignant distal biliary obstructions: a prospective randomized trial, Gastrointest. Endosc. (2023).
[18] C. Vaishnavi, J. Samanta, R. Kochhar, Characterization of biofilms in biliary stents and potential factors involved in occlusion, World J. Gastroenterol. 24 (1) (2018) 112–123.
[19] F. Ahadi, M. Azadi, M. Biglari, et al., Evaluation of coronary stents: a review of types, materials, processing techniques, design, and problems, Heliyon 9 (2) (2023) e13575.
[20] H.S. Nam, D.H. Kang, Current status of biliary metal stents, Clin. Endosc. 49 (2) (2016) 124–130.
[21] E. Fuentes-Valenzuela, M. de Benito Sanz, F. García-Pajares, et al., Antimigration versus conventional fully covered metal stents in the endoscopic treatment of anastomotic biliary strictures after deceased-donor liver transplantation, Surg. Endosc. 37 (9) (2023) 6975–6982.
[22] G. Vanella, C. Coluccio, A. Cucchetti, et al., Fully covered versus partially covered self-expandable metal stents for palliation of distal malignant biliary obstruction: a systematic review and meta-analysis, Gastrointest. Endosc. 99 (3) (2024).
[23] C.H. Park, S.W. Park, J.H. Jung, et al., Comparative efficacy of various stents for palliation in patients with malignant extrahepatic biliary obstruction: a systematic review and network meta-analysis, J. Personalized Med. 11 (2) (2021).
[24] K. Kataoka, H. Kawashima, E. Ohno, et al., Comparison of outcomes between secondary fully covered and uncovered self-expandable metal stents in the treatment of recurrent biliary obstruction of pancreatic cancer, Surg, Endoscopy 36 (8) (2022) 5676–5683.
[25] Y. Yamashita, A. Tachikawa, T. Shimokawa, et al., Covered versus uncovered metal stent for endoscopic drainage of a malignant distal biliary obstruction: meta-analysis, Dig. Endosc. 34 (5) (2022) 938–951.
[26] S.E. Ali, W.M. Frandah, L. Su, et al., Should a fully covered self-expandable biliary metal stent be anchored with a double-pigtail plastic stent? A retrospective study, World J. Gastrointest. Endosc 11 (5) (2019) 365–372.
[27] J.J. Telford, D.L. Carr-Locke, T.H. Baron, et al., A randomized trial comparing uncovered and partially covered self-expandable metal stents in the palliation of distal malignant biliary obstruction, Gastrointest. Endosc. 72 (5) (2010) 907–914.
[28] N.T. Nguyen, H.A. Khan, K. Abdul-Baki, et al., CT imaging features of bile duct stent complications, Clin. Imag. 103 (2023) 109986.
[29] J. Hur, W. Choi, S.L. Choi, et al., Percutaneous placement of a retrievable fully covered metal stent with anchoring flaps for the treatment of biliary anastomotic stricture following LDLT, J. Int. Med. Res. 52 (3) (2024) 3000605241239215.
[30] F. Brinkmann, K. Uhlig, A. Sambale, et al., Anchoring fins of fully covered self-expandable metal stents affect pull-out force and stent migration, Gastrointest. Endosc. 99 (3) (2024) 377–386.e373.
[31] M. Miyazawa, H. Takatori, H. Okafuji, et al., Efficacy of a novel self-expandable metal stent with dumbbell-shaped flare ends for distal biliary obstruction due to unresectable pancreatic cancer, Sci. Rep. 12 (1) (2022) 21100.
[32] J.W. Chun, S.M. Woo, M. Han, et al., Prolonged patency of fully covered self-expandable metal stents with an externally anchored plastic stent in distal malignant biliary obstruction, Endoscopy 55 (6) (2023) 563–568.
[33] S. Kulpatcharapong, P. Piyachaturawat, P. Mekaroonkamol, et al., Efficacy of multi-hole self-expandable metal stent compared to fully covered and uncovered

self-expandable metal stents in patients with unresectable malignant distal biliary obstruction: a propensity analysis, Surg. Endosc. 37 (12) (2023) 9062–9069.
[34] G. Li, M. Zhao, F. Xu, et al., Synthesis and biological application of polylactic acid, Molecules 25 (21) (2020).
[35] A. Siiki, R. Jesenofsky, M. Löhr, et al., Biodegradable biliary stents have a different effect than covered metal stents on the expression of proteins associated with tissue healing in benign biliary strictures, Scand. J. Gastroenterol. 51 (7) (2016) 880–885.
[36] S.-W. Baek, J.H. Kim, D.H. Song, et al., Enhanced mechanical properties and anti–inflammation of poly(L–lactic acid) by stereocomplexes of PLLA/PDLA and surface–modified magnesium hydroxide nanoparticles, Polymers 14 (18) (2022) 3790.
[37] B. Meng, J. Wang, N. Zhu, et al., Study of biodegradable and self-expandable PLLA helical biliary stent in vivo and in vitro, Journal of materials science, J. Mater. Sci. Mater. Med. 17 (7) (2006) 611–617.
[38] K. Yamamoto, T. Yoshioka, K. Furuichi, et al., Experimental study of poly-L-lactic acid biodegradable stents in normal canine bile ducts, Cardiovasc. Intervent. Radiol. 34 (3) (2011) 601–608.
[39] A.M. Sousa, A.M. Amaro, A.P. Piedade, 3D printing of polymeric bioresorbable stents: a strategy to improve both cellular compatibility and mechanical properties, Polymers (Basel) 14 (6) (2022).
[40] J. Manzur, M. Akhtar, A. Aizaz, et al., Electrophoretic deposition, microstructure, and selected properties of poly(lactic-co-glycolic) acid-based antibacterial coatings on Mg substrate, ACS Omega 8 (20) (2023) 18074–18089.
[41] Y. Lu, D. Cheng, B. Niu, et al., Properties of poly (Lactic-co-Glycolic acid) and progress of poly (Lactic-co-Glycolic acid)-based biodegradable materials in biomedical research, Pharmaceuticals 16 (3) (2023) 454.
[42] W. Xu, M. Sasaki, T. Niidome, Sirolimus release from biodegradable polymers for coronary stent application: a review, Pharmaceutics 14 (3) (2022).
[43] X. Xu, T. Liu, K. Zhang, et al., Biodegradation of poly(l-lactide-co-glycolide) tube stents in bile, Polym. Degrad. Stabil. 93 (4) (2008) 811–817.
[44] X. Xu, T. Liu, S. Liu, et al., Feasibility of biodegradable PLGA common bile duct stents: an in vitro and in vivo study, J. Mater. Sci. Mater. Med. 20 (5) (2009) 1167–1173.
[45] J.A. Martins, A.A. Lach, H.L. Morris, et al., Polydioxanone implants: a systematic review on safety and performance in patients, J. Biomater. Appl. 34 (7) (2020) 902–916.
[46] J. Petrtýl, R. Brůha, L. Horák, et al., Management of benign intrahepatic bile duct strictures: initial experience with polydioxanone biodegradable stents, Endoscopy 42 (Suppl 2) (2010) E89–90.
[47] G. Mauri, C. Michelozzi, F. Melchiorre, et al., Biodegradable biliary stent implantation in the treatment of benign bilioplastic-refractory biliary strictures: preliminary experience, Eur. Radiol. 23 (12) (2013) 3304–3310.
[48] L. Jones, J. Moir, C. Brown, et al., The novel use of a biodegradable stent placed by percutaneous transhepatic cholangiography for the treatment of a hepaticojejunostomy biliary leak following an extended left hepatectomy and pancreaticoduodenectomy, Ann. R. Coll. Surg. Engl. 96 (6) (2014) e1–e3.
[49] G. Mauri, C. Michelozzi, F. Melchiorre, et al., Benign biliary strictures refractory to standard bilioplasty treated using polydoxanone biodegradable biliary stents: retrospective multicentric data analysis on 107 patients, Eur. Radiol. 26 (11) (2016) 4057–4063.
[50] A. Siiki, I. Rinta-Kiikka, J. Sand, et al., Biodegradable biliary stent in the endoscopic treatment of cystic duct leak after cholecystectomy: the first case report and review of literature, J. Laparoendosc. Adv. Part A 25 (5) (2015) 419–422.
[51] D. Mullan, D. Shepherd, H.-U. Laasch, Percutaneous biodegradable stent insertion for a benign biliary stricture complicating choledochojejunostomy, Gastrointest. Interv. 4 (1) (2015) 58–60.
[52] T. Grolich, M. Crha, L. Novotný, et al., Self-expandable biodegradable biliary stents in porcine model, J. Surg. Res. 193 (2) (2015) 606–612.
[53] S. Sánchez-Cabús, D. Calatayud, J. Ferrer, et al., Beneficial effect of a resorbable biliary stent in living donor liver transplantation, Eur. Surg. Res. 56 (3–4) (2016) 123–131.
[54] L. Janousek, S. Maly, M. Oliverius, et al., Bile duct anastomosis supplied with biodegradable stent in liver transplantation: the initial experience, transplant, SAVE Proc. 48 (10) (2016) 3312–3316.
[55] M.E. Giménez, M. Palermo, E. Houghton, et al., Biodegradable biliary stents: a new approach for the management of hepaticojejunostomy strictures following bile duct injury. Prospective study, ABCD-Arq. Bras. Cir. Dig.-Braz. Arch. Dig. Surg. 29 (2) (2016) 112–116.
[56] A. Siiki, I. Rinta-Kiikka, J. Sand, et al., Endoscopic biodegradable biliary stents in the treatment of benign biliary strictures: first report of clinical use in patients, Dig. Endosc. 29 (1) (2017) 118–121.
[57] A. Siiki, I. Rinta-Kiikka, J. Sand, et al., A pilot study of endoscopically inserted biodegradable biliary stents in the treatment of benign biliary strictures and cystic duct leaks, Gastrointest. Endosc. 87 (4) (2018) 1132–1137.
[58] C. Dopazo, I. Diez, J. Quintero, et al., Role of biodegradable stents as part of treatment of biliary strictures after pediatric and adult liver transplantation: an observational single-center study, J. Vasc. Intervent. Radiol. 29 (6) (2018) 899–904.
[59] M. Battistel, M. Senzolo, A. Ferrarese, et al., Biodegradable biliary stents for percutaneous treatment of post-liver transplantation refractory benign biliary anastomotic strictures, Cardiovasc. Intervent. Radiol. 43 (5) (2020) 749–755.
[60] A. Anderloni, A. Fugazza, L. Maroni, et al., New biliary and pancreatic biodegradable stent placement: a single-center, prospective, pilot study (with video), Gastrointest. Endosc. 92 (2) (2020) 405–411.
[61] W. Wang, Z. Luan, Z. Shu, et al., Biosynthetic plastics as tunable elastic and visible stent with shape-memory to treat biliary stricture, Adv. Sci. (Weinh) 10 (29) (2023) e2303779.
[62] O.S. Obisesan, T.O. Ajiboye, S.D. Mhlanga, et al., Biomedical applications of biodegradable polycaprolactone-functionalized magnetic iron oxides nanoparticles and their polymer nanocomposites, Colloid Surf. B-Biointerfaces 227 (2023) 113342.
[63] P.R. Schmitt, K.D. Dwyer, K.L.K. Coulombe, Current applications of polycaprolactone as a scaffold material for heart regeneration, ACS Appl. Bio Mater. 5 (6) (2022) 2461–2480.
[64] H. Tashiro, T. Ogawa, T. Itamoto, et al., Synthetic bioabsorbable stent material for duct-to-duct biliary reconstruction, J. Surg. Res. 151 (1) (2009) 85–88.
[65] T. Itoi, K. Kasuya, Y. Abe, et al., Endoscopic placement of a new short-term biodegradable pancreatic and biliary stent in an animal model: a preliminary feasibility study (with videos), J. Hepato-Biliary-Pancreatic Sci. 18 (3) (2011) 463–467.
[66] A. Seyedsalehi, L. Daneshmandi, M. Barajaa, et al., Fabrication and characterization of mechanically competent 3D printed polycaprolactone-reduced graphene oxide scaffolds, Sci. Rep. 10 (1) (2020) 22210.
[67] H. Emadi, M. Karevan, M. Masoudi Rad, et al., Bioactive and biodegradable polycaprolactone-based nanocomposite for bone repair applications, Polymers 15 (17) (2023) 3617.
[68] B.L. Pereira, V.S. Sampaio, G.G. de Lima, et al., Biomedical applications of polyvinyl alcohol-based bionanocomposites. Polyvinyl Alcohol-Based Biocomposites and Bionanocomposites, 2023, pp. 179–203.
[69] M. Wang, J. Bai, K. Shao, et al., Poly(vinyl alcohol) hydrogels: the old and new functional materials, Int. J. Polym. Sci. 2021 (2021) 2225426.
[70] Y. Nagakawa, S. Fujita, S. Yunoki, et al., Self-expandable hydrogel biliary stent design utilizing the swelling property of poly(vinyl alcohol) hydrogel, J. Appl. Polym. Sci. 137 (28) (2020) 48851.
[71] Y. Nagakawa, S. Fujita, S. Yunoki, et al., Characterization and preliminary in vivo evaluation of a self-expandable hydrogel stent with anisotropic swelling behavior and endoscopic deliverability for use in biliary drainage, J. Mater. Chem. B 10 (23) (2022) 4375–4385.
[72] D.D. Pedersen, S. Kim, W.R. Wagner, Biodegradable polyurethane scaffolds in regenerative medicine: clinical translation review, J. Biomed. Mater. Res., Part A 110 (8) (2022) 1460–1487.
[73] C.I. Kwon, J.S. Son, K.S. Kim, et al., Mechanical properties and degradation process of biliary self-expandable biodegradable stents, Dig. Endosc. 33 (7) (2021) 1158–1169.
[74] Y. Zhu, K. Yang, R. Cheng, et al., The current status of biodegradable stent to treat benign luminal disease, Mater. Today 20 (9) (2017) 516–529.
[75] G. Ginsberg, C. Cope, J. Shah, et al., In vivo evaluation of a new bioabsorbable self-expanding biliary stent, Gastrointest. Endosc. 58 (5) (2003) 777–784.
[76] J. Laukkarinen, I. Nordback, J. Mikkonen, et al., A novel biodegradable biliary stent in the endoscopic treatment of cystic-duct leakage after cholecystectomy, Gastrointest. Endosc. 65 (7) (2007) 1063–1068.
[77] J.M. Laukkarinen, J.A. Sand, P. Chow, et al., A novel biodegradable biliary stent in the normal duct hepaticojejunal anastomosis: an 18-month follow-up in a large animal model, J. Gastrointest. Surg. 11 (6) (2007) 750–757.
[78] J. Laukkarinen, J. Sand, J. Leppiniemi, et al., A novel technique for hepaticojejunostomy for nondilated bile ducts: a purse-string anastomosis with an intra-anastomotic biodegradable biliary stent, Am. J. Surg. 200 (1) (2010) 124–130.
[79] K. Yamamoto, T. Yoshioka, K. Furuichi, et al., Experimental study of poly-L-lactic acid biodegradable stents in normal canine bile ducts, Cardiovasc. Intervent. Radiol. 34 (3) (2011) 601–608.
[80] A. Oñate, T. Sáez-Llanos, A. Jaramillo, et al., Enhancing mechanical properties of PLA and PP composites through ionic zeolite with copper nanoparticle reinforcement: microstructural and micromechanical characterization, Int. J. Adv. Manuf. Technol. 129 (7) (2023) 3375–3386.
[81] E. Girard, G. Chagnon, A. Moreau-Gaudry, et al., Evaluation of a biodegradable PLA-PEG-PLA internal biliary stent for liver transplantation: in vitro degradation and mechanical properties, J. Biomed. Mater. Res., Part B 109 (3) (2021) 410–419.
[82] S. Liu, S. He, C. Chen, et al., A versatile disorder-to-order technology to upgrade polymers into high-performance bioinspired materials, Adv. Healthcare Mater. 12 (22) (2023) 2300068.
[83] J. Zan, G. Qian, F. Deng, et al., Dilemma and breakthrough of biodegradable poly-l-lactic acid in bone tissue repair, J. Mater. Res. Technol. 17 (2022) 2369–2387.
[84] N. Yahyaee, A. Javadi, H. Garmabi, et al., Effect of two-step chain extension using joncryl and PMDA on the rheological properties of poly (lactic acid), Macromol. Mater. Eng. 305 (2) (2020) 1900423.
[85] J. Lu, Z. Qiu, W. Yang, Fully biodegradable blends of poly(l-lactide) and poly (ethylene succinate): miscibility, crystallization, and mechanical properties, Polymer 48 (14) (2007) 4196–4204.
[86] A. Pei, Q. Zhou, L.A. Berglund, Functionalized cellulose nanocrystals as biobased nucleation agents in poly(l-lactide) (PLLA) – crystallization and mechanical property effects, Compos. Sci. Technol. 70 (5) (2010) 815–821.
[87] X. Dai, Y. Cao, X. Shi, et al., The PLA/ZIF-8 nanocomposite membranes: the diameter and surface roughness adjustment by ZIF-8 nanoparticles, high wettability, improved mechanical property, and efficient oil/water separation, Adv. Mater. Interfac. 3 (24) (2016) 1600725.
[88] M. Asadniaye Fardjahromi, H. Nazari, S.M. Ahmadi Tafti, et al., Metal-organic framework-based nanomaterials for bone tissue engineering and wound healing, Mater. Today Chem. 23 (2022) 100670.

[89] H. Wang, Z. Fu, W. Dong, et al., Formation of interfacial janus nanomicelles by reactive blending and their compatibilization effects on immiscible polymer blends, J. Phys. Chem. B 120 (34) (2016) 9240–9252.
[90] J. Nam, Y. Song, Preparation and analysis of biodegradable polydioxanone/chitosan film, J. Polym. Res. 29 (2022).
[91] X. Liu, S. Feng, X. Wang, et al., Tuning the mechanical properties and degradation properties of polydioxanone isothermal annealing, Turk. J. Chem. 44 (5) (2020) 1430–1444.
[92] H.b. Hashim, N.A.A.b. Emran, T. Isono, et al., Improving the mechanical properties of polycaprolactone using functionalized nanofibrillated bacterial cellulose with high dispersibility and long fiber length as a reinforcement material, Compos. Appl. Sci. Manuf. 158 (2022) 106978.
[93] Y. Zhang, P.a. Song, H. Liu, et al., Morphology, healing and mechanical performance of nanofibrillated cellulose reinforced poly(ε-caprolactone)/epoxy composites, Compos. Sci. Technol. 125 (2016) 62–70.
[94] X.-L. Hu, S. Mi, J.-L. Lu, et al., In vitro degradation behavior of shape memory PLLA-TMC random copolymers, Colloid Surf. A-Physicochem. Eng. Asp. 615 (2021) 126220.
[95] C. Shuai, J. Zan, F. Qi, et al., nMgO-incorporated PLLA bone scaffolds: enhanced crystallinity and neutralized acidic products, Mater. Des. 174 (2019) 107801.
[96] R. Mahar, A. Chakraborty, N. Nainwal, et al., Application of PLGA as a biodegradable and biocompatible polymer for pulmonary delivery of drugs, AAPS PharmSciTech 24 (1) (2023) 39.
[97] C. Zhao, H. Wu, J. Ni, et al., Development of PLA/Mg composite for orthopedic implant: tunable degradation and enhanced mineralization, Compos. Sci. Technol. 147 (2017) 8–15.
[98] M. Li, H. Yuan, W. Ding, et al., Selective laser sintering PLA/Mg composite scaffold with promoted degradation and enhanced mechanical, J. Polym. Environ. (2024).
[99] T.O. Xu, H.S. Kim, T. Stahl, et al., Self-neutralizing PLGA/magnesium composites as novel biomaterials for tissue engineering, Biomed. Mater. 13 (3) (2018) 035013.
[100] P. Wan, C. Yuan, L. Tan, et al., Fabrication and evaluation of bioresorbable PLLA/magnesium and PLLA/magnesium fluoride hybrid composites for orthopedic implants, Compos. Sci. Technol. 98 (2014) 36–43.
[101] L. He, X. Liu, C. Rudd, Additive-manufactured gyroid scaffolds of magnesium oxide, phosphate glass fiber and polylactic acid composite for bone tissue engineering, Polymers (Basel) 13 (2) (2021).
[102] Y. Zhao, H. Liang, S. Zhang, et al., Effects of magnesium oxide (MgO) shapes on in vitro and in vivo degradation behaviors of PLA/MgO composites in long term, Polymers (Basel) 12 (5) (2020).
[103] X. Liu, X. He, D. Jin, et al., A biodegradable multifunctional nanofibrous membrane for periodontal tissue regeneration, Acta Biomater. 108 (2020) 207–222.
[104] W. Guo, W. Bu, Y. Mao, et al., Magnesium hydroxide as a versatile nanofiller for 3D-printed PLA bone scaffolds, Polymers 16 (2) (2024) 198.
[105] J.-K. Kim, E.-J. Go, K.-W. Ko, et al., PLGA microspheres containing hydrophobically modified magnesium hydroxide particles for acid neutralization-mediated anti-inflammation, Tissue Eng. Regen. Med. 18 (4) (2021) 613–622.
[106] S.K. Lee, C.-M. Han, W. Park, et al., Synergistically enhanced osteoconductivity and anti-inflammation of PLGA/β-TCP/Mg(OH)2 composite for orthopedic applications, Mater. Sci. Eng., C 94 (2019) 65–75.
[107] C.H. Kum, Y. Cho, Y.K. Joung, et al., Biodegradable poly(l-lactide) composites by oligolactide-grafted magnesium hydroxide for mechanical reinforcement and reduced inflammation, J. Mater. Chem. B 1 21 (2013) 2764–2772.
[108] Y. Xiao, Y.n. Yang, J. Li, et al., Porous composite calcium citrate/polylactic acid materials with high mineralization activity and biodegradability for bone repair tissue engineering, Int. J. Polym. Mater. Polym. Biomat. 70 (2020) 507–520.
[109] M. Bartnikowski, T.R. Dargaville, S. Ivanovski, et al., Degradation mechanisms of polycaprolactone in the context of chemistry, geometry and environment, Prog. Polym. Sci. 96 (2019) 1–20.
[110] G. Padmore, F.R. Sutherland, C.G. Ball, The art and craft of biliary T-tube Use, J. Trauma Acute Care Surg. 91 (2) (2021) e46–e49.
[111] S. Daldoul, A. Moussi, A. Zaouche, T-tube drainage of the common bile duct choleperitoneum: etiology and management, J. Vis. Surg. 149 (3) (2012) e172–e178.
[112] Y. Yu, S.-J. Zhu, H.-T. Dong, et al., A novel MgF2/PDA/S-HA coating on the biodegradable ZE21B alloy for better multi-functions on cardiovascular application, J. Magnesium Alloys 11 (2) (2023) 480–492.
[113] Y. Chen, J. Yan, Z. Wang, et al., In vitro and in vivo corrosion measurements of Mg-6Zn alloys in the bile, Mater. Sci. Eng., C 42 (2014) 116–123.
[114] Y. Chen, J. Yan, X. Wang, et al., In vivo and in vitro evaluation of effects of Mg-6Zn alloy on apoptosis of common bile duct epithelial cell, Biometals 27 (6) (2014) 1217–1230.
[115] Y. Liu, S. Zheng, N. Li, et al., In vivo response of AZ31 alloy as biliary stents: a 6 months evaluation in rabbits, Sci. Rep. 7 (2017) 40184.
[116] T. Li, W. Xu, C. Liu, et al., Anticancer effect of biodegradable magnesium on hepatobiliary carcinoma: an in vitro and in vivo study, ACS Biomater. Sci. Eng. 7 (6) (2021) 2774–2782.
[117] H. Peng, K. Fan, R. Zan, et al., Degradable magnesium implants inhibit gallbladder cancer, Acta Biomater. 128 (2021) 514–522.
[118] N.G. Khouri, J.O. Bahú, C. Blanco-Llamero, et al., Polylactic acid (PLA): properties, synthesis, and biomedical applications – a review of the literature, J. Mol. Struct. 1309 (2024) 138243.
[119] J. Chen, L. Tan, X. Yu, et al., Mechanical properties of magnesium alloys for medical application: a review, J. Mech. Behav. Biomed. Mater. 87 (2018) 68–79.
[120] M. Ali, M.A. Hussein, N. Al-Aqeeli, Magnesium-based composites and alloys for medical applications: a review of mechanical and corrosion properties, J. Alloys Compd. 792 (2019) 1162–1190.
[121] W. Yamagata, T. Fujisawa, T. Sasaki, et al., Evaluation of the mechanical properties of current biliary self-expandable metallic stents: axial and radial force, and axial force zero border, Clin. Endosc. 56 (5) (2023) 633–649.
[122] K. Yuan, C. Deng, L. Tan, et al., Structural and temporal dynamics analysis of zinc-based biomaterials: history, research hotspots and emerging trends, Bioact. Mater. 35 (2024) 306–329.
[123] C. Zhou, H.F. Li, Y.X. Yin, et al., Long-term in vivo study of biodegradable Zn-Cu stent: a 2-year implantation evaluation in porcine coronary artery, Acta Biomater. 97 (2019) 657–670.
[124] S. Jha, R. Rani, S. Singh, Biogenic zinc oxide nanoparticles and their biomedical applications: a review, J. Inorg. Organomet. Polym. Mater. 33 (6) (2023) 1437–1452.
[125] M. Vithayathil, S.A. Khan, Current epidemiology of cholangiocarcinoma in Western countries, J. Hepatol. 77 (6) (2022) 1690–1698.
[126] Y. Li, J. Yu, Y. Zhang, et al., Advances in targeted therapy of cholangiocarcinoma, Ann. Med. 56 (1) (2024) 2310196.
[127] S.A. Khan, B.R. Davidson, R. Goldin, et al., Guidelines for the diagnosis and treatment of cholangiocarcinoma: consensus document, Gut 51 (suppl 6) (2002) vi1–vi9.
[128] Q. Shang, Y. Dong, Y. Su, et al., Local scaffold-assisted delivery of immunotherapeutic agents for improved cancer immunotherapy, Adv. Drug Deliv. Rev. 185 (2022) 114308.
[129] S. Mezawa, H. Homma, T. Sato, et al., A study of carboplatin-coated tube for the unresectable cholangiocarcinoma, Hepatology 32 (5) (2000) 916–923.
[130] D.K. Lee, H.S. Kim, K.S. Kim, et al., The effect on porcine bile duct of a metallic stent covered with a paclitaxel-incorporated membrane, Gastrointest. Endosc. 61 (2) (2005) 296–301.
[131] S.I. Jang, J.H. Kim, M. Kim, et al., Porcine feasibility and safety study of a new paclitaxel-eluting biliary stent with a Pluronic-containing membrane, Endoscopy 44 (9) (2012) 825–831.
[132] J.W. Lee, S.G. Yang, K. Na, Gemcitabine-releasing polymeric films for covered self-expandable metallic stent in treatment of gastrointestinal cancer, Int. J. Pharmacol. 427 (2) (2012) 276–283.
[133] D.H. Kim, Y.I. Jeong, C.W. Chung, et al., Preclinical evaluation of sorafenib-eluting stent for suppression of human cholangiocarcinoma cells, Int. J. Nanomed. 8 (2013) 1697–1711.
[134] T.W. Kwak, H.L. Lee, Y.H. Song, et al., Vorinostat-eluting poly(DL-lactide-co-glycolide) nanofiber-coated stent for inhibition of cholangiocarcinoma cells, Int. J. Nanomed. 12 (2017) 7669–7680.
[135] M. Chen, C. Qian, B. Jin, et al., Curcumin analog WZ26 induces ROS and cell death via inhibition of STAT3 in cholangiocarcinoma, Cancer Biol. Ther. 24 (1) (2023) 2162807.
[136] H.H. Jang, S.B. Park, J.S. Hong, et al., Piperlongumine-eluting gastrointestinal stent using reactive oxygen species-sensitive nanofiber mats for inhibition of cholangiocarcinoma cells, Nanoscale Res. Lett. 14 (1) (2019) 58.
[137] P. Gentile, I. Carmagnola, T. Nardo, et al., Layer-by-layer assembly for biomedical applications in the last decade, Nanotechnology 26 (42) (2015) 422001.
[138] M. Zhianmanesh, A. Gilmour, M.M.M. Bilek, et al., Plasma surface functionalization: a comprehensive review of advances in the quest for bioinstructive materials and interfaces, Appl. Phys. Rev. 10 (2) (2023).
[139] P. Amrollahi, J.S. Krasinski, R. Vaidyanathan, et al., Electrophoretic deposition (EPD): fundamentals and applications from nano- to microscale structures, in: M. Aliofkhazraei, A.S.H. Makhlouf (Eds.), Handbook of Nanoelectrochemistry: Electrochemical Synthesis Methods, Properties, and Characterization Techniques, Springer International Publishing, Cham, 2016, pp. 561–591.
[140] X. Feng, J. Li, X. Zhang, et al., Electrospun polymer micro/nanofibers as pharmaceutical repositories for healthcare, J. Contr. Release 302 (2019) 19–41.
[141] J.B. Xiao, J.Y. Weng, Y.Y. Hu, et al., Feasibility and efficacy evaluation of metallic biliary stents eluting gemcitabine and cisplatin for extrahepatic cholangiocarcinoma, World J. Gastroenterol. 26 (31) (2020) 4589–4606.
[142] D. Yun, H.O. Kim, H.Y. Son, et al., Stent containing CD44-targeting polymeric prodrug nanoparticles that release paclitaxel and gemcitabine in a time interval-controlled manner for synergistic human biliary cancer therapy, J. Mater. Chem. B 5 (31) (2017) 6317–6324.
[143] J. Xu, C. Yang, Cholecystectomy outcomes after endoscopic sphincterotomy in patients with choledocholithiasis: a meta-analysis, BMC Gastroenterol. 20 (1) (2020) 229.
[144] M. Manti, J. Shah, A. Papaefthymiou, et al., Endoscopic management of difficult biliary stones: an evergreen issue, Medicina 60 (2) (2024).
[145] S. Terada, S. Kawaguchi, E. Nakatani, et al., Prospective study on planned biliary stent placement to treat small common bile duct stones, JGH Open 8 (2) (2024) e13040.
[146] X.B. Cai, W.X. Zhang, X.J. Wan, et al., The effect of a novel drug-eluting plastic stent on biliary stone dissolution in an ex vivo bile perfusion model, Gastrointest. Endosc. 79 (1) (2014) 156–162.
[147] X.B. Cai, W.X. Zhang, R.L. Zhang, et al., Safety and efficacy of a novel plastic stent coated with stone-dissolving agents for the treatment of biliary stones in a porcine model, Endoscopy 47 (5) (2015) 457–461.
[148] Q. Gao, C. Huang, B. Sun, et al., Fabrication and characterization of metal stent coating with drug-loaded nanofiber film for gallstone dissolution, J. Biomater. Appl. 31 (5) (2016) 784–796.

[149] C. Huang, X.B. Cai, L.L. Guo, et al., Drug-eluting fully covered self-expanding metal stent for dissolution of bile duct stones in vitro, World J. Gastroenterol. 25 (26) (2019) 3370–3379.
[150] Y. Wang, J. Jia, B. Qian, et al., New type of electrospinning drug-loaded nanofiber membrane in the treatment of gallstone disease, Appl. Nanosci. 13 (5) (2023) 3523–3531.
[151] V. Sebghatollahi, M. Parsa, M. Minakari, et al., A clinician's guide to gallstones and common bile duct (CBD): a study protocol for a systematic review and evidence-based recommendations, Health Sci. Rep. 6 (9) (2023) e1555.
[152] F. Grünhage, F. Lammert, Pathogenesis of gallstones: a genetic perspective, Best Pract. Res. Clin. Gastroenterol. 20 (6) (2006) 997–1015.
[153] T. Wu, Y. Yang, H. Su, et al., Recent developments in antibacterial or antibiofilm compound coating for biliary stents, Colloid Surf. B-Biointerfaces 219 (2022) 112837.
[154] T. Wuestefeld, C. Klein, K.L. Streetz, et al., Lack of gp130 expression results in more bacterial infection and higher mortality during chronic cholestasis in mice, Hepatology 42 (5) (2005) 1082–1090. Baltimore, Md.
[155] K.Y. Kim, J. Han, H.G. Kim, et al., Late complications and stone recurrence rates after bile duct stone removal by endoscopic sphincterotomy and large balloon dilation are similar to those after endoscopic sphincterotomy alone, Clin. Endosc. 46 (6) (2013) 637–642.
[156] S. Zhao, J. Wang, J. Ge, et al., Implantation of covered self-expandable metal stent in the common bile duct for the treatment of choledochoduodenal fistula, J. Clin. Gastroenterol. 48 (4) (2014) 383–384.
[157] T. Hamada, Y. Nakai, H. Isayama, et al., Antireflux metal stent for biliary obstruction: any benefits? Dig. Endosc. 33 (3) (2021) 310–320.
[158] Y. Su, Z. Xiang, X. Song, et al., Design and optimization of a new anti-reflux biliary stent with retractable bionic valve based on fluid-structure interaction analysis, Front. Bioeng. Biotechnol. 10 (2022) 824207.
[159] Y. Wang, X.-F. Song, Y.-S. Su, et al., Design and evaluation of a novel anti-reflux biliary stent with cone spiral valve, Proc. Inst. Mech. Eng. Part H-J. Eng. Med. 235 (1) (2020) 54–64.
[160] K. Sauer, P. Stoodley, D.M. Goeres, et al., The biofilm life cycle: expanding the conceptual model of biofilm formation, Nat. Rev. Microbiol. 20 (10) (2022) 608–620.
[161] L.K. Vestby, T. Grønseth, R. Simm, et al., Bacterial biofilm and its role in the pathogenesis of disease, Antibiotics 9 (2) (2020).
[162] A. Kaushal, I. Khurana, P. Yadav, et al., Advances in therapeutic applications of silver nanoparticles, Chem. Biol. Interact. 382 (2023) 110590.
[163] F. Yang, Z. Ren, Q. Chai, et al., A novel biliary stent coated with silver nanoparticles prolongs the unobstructed period and survival via anti-bacterial activity, Sci. Rep. 6 (2016) 21714.
[164] A. Yamabe, A. Irisawa, I. Wada, et al., Application of a silver coating on plastic biliary stents to prevent biofilm formation: an experimental study using electron microscopy, Endosc. Int. Open 4 (10) (2016) E1090–e1095.
[165] Y. Tian, M. Xia, S. Zhang, et al., Initial study of sediment antagonism and characteristics of silver nanoparticle-coated biliary stents in an experimental animal model, Int. J. Nanomed. 11 (2016) 1807–1817.
[166] W. Wen, L.M. Ma, W. He, et al., Silver-nanoparticle-coated biliary stent inhibits bacterial adhesion in bacterial cholangitis in swine, Hepatobiliary Pancreat. Dis. Int. 15 (1) (2016) 87–92.
[167] H. Khizar, Y. Hu, Y. Wu, et al., Efficacy and safety of radiofrequency ablation plus stent versus stent-alone treatments for malignant biliary strictures: a systematic review and meta-analysis, J. Clin. Gastroenterol. 57 (4) (2023) 335–345.
[168] M. de Oliveira Veras, D.T.H. de Moura, T.R. McCarty, et al., Intraductal radiofrequency ablation plus biliary stent versus stent alone for malignant biliary obstruction: a systematic review and meta-analysis, Endosc. Int. Open 12 (1) (2024) E23–e33.
[169] Y. Park, D.S. Won, G.H. Bae, et al., Silver nanofunctionalized stent after radiofrequency ablation suppresses tissue hyperplasia and bacterial growth, Pharmaceutics 14 (2) (2022).
[170] W. Park, K.Y. Kim, J.M. Kang, et al., Metallic stent mesh coated with silver nanoparticles suppresses stent-induced tissue hyperplasia and biliary sludge in the rabbit extrahepatic bile duct, Pharmaceutics 12 (6) (2020).
[171] L. Xu, Y.Y. Wang, J. Huang, et al., Silver nanoparticles: synthesis, medical applications and biosafety, Theranostics 10 (20) (2020) 8996–9031.
[172] J. Zhang, F. Wang, S.S.K. Yalamarty, et al., Nano silver-induced toxicity and associated mechanisms, Int. J. Nanomed. 17 (2022) 1851–1864.
[173] B. Zhang, N. Liu, Q.S. Liu, et al., Silver nanoparticles induce size-dependent and particle-specific neurotoxicity to primary cultures of rat cerebral cortical neurons, Ecotoxicol. Environ. Saf. 198 (2020) 110674.
[174] A. Al-Doaiss, Q. Jarrar, S. Moshawih, Hepatic histopathological and ultrastructural alterations induced by 10 nm silver nanoparticles, IET Nanobiotechnol. 14 (5) (2020) 405–411.
[175] L.Q. Chen, L. Fang, J. Ling, et al., Nanotoxicity of silver nanoparticles to red blood cells: size dependent adsorption, uptake, and hemolytic activity, Chem. Res. Toxicol. 28 (3) (2015) 501–509.
[176] B. Das, S. Tripathy, J. Adhikary, et al., Surface modification minimizes the toxicity of silver nanoparticles: an in vitro and in vivo study, J. Biol. Inorg. Chem. 22 (6) (2017) 893–918.
[177] E. Madla-Cruz, M. De la Garza-Ramos, C.I. Romo-Sáenz, et al., Antimicrobial activity and inhibition of biofilm formation in vitro and on human dentine by silver nanoparticles/carboxymethyl-cellulose composites, Arch. Oral Biol. 120 (2020) 104943.
[178] E.M. Lee, J. Lee, Y. Kim, et al., Hybrid composite of silver nanoparticle–porous silicon microparticles as an image-guided localization agent for computed tomography scan of the lungs, ACS Biomater. Sci. Eng. 6 (8) (2020) 4390–4396.
[179] Z. Yu, W. Wang, F. Kong, et al., Cellulose nanofibril/silver nanoparticle composite as an active food packaging system and its toxicity to human colon cells, Int. J. Biol. Macromol. 129 (2019) 887–894.
[180] J. E de la Cruz Conty, A. Budía Alba, J.L. Sanz Migueláñez, et al., Heparin as an antibacterial coating on biodegradable ureteral stents: experimental study of BRAIDSTENT®-H, Br. J. Surg. 108 (Supplement_3) (2021).
[181] C. Guarise, M. Maglio, M. Sartori, et al., Titanium implant coating based on dopamine-functionalized sulphated hyaluronic acid: in vivo assessment of biocompatibility and antibacterial efficacy, Mater. Sci. Eng., C 128 (2021) 112286.
[182] F. Cetta, R. Rappuoli, G. Montalto, et al., New biliary endoprosthesis less liable to block in biliary infections: description and in vitro studies, Eur. J. Surg. 165 (8) (1999) 782–785.
[183] M.-C. Peng, J.-C. Lin, C.-Y. Chen, et al., Studies of sulfonated polyethylene for biliary stent application, J. Appl. Polym. Sci. 92 (4) (2004) 2450–2457.
[184] M.J. Farnbacher, R. Lederer, A. Blana, et al., Does heparin coating reduce encrustation of biliary plastic endoprostheses? A prospective randomized trial, Scand. J. Gastroenterol. 47 (10) (2012) 1141–1147.
[185] S. Zheng, M. Bawazir, A. Dhall, et al., Implication of surface properties, bacterial motility, and hydrodynamic conditions on bacterial surface sensing and their initial adhesion, Front. Bioeng. Biotechnol. 9 (2021) 643722.
[186] K. Yang, J. Shi, L. Wang, et al., Bacterial anti-adhesion surface design: surface patterning, roughness and wettability: a review, J. Mater. Sci. Technol. 99 (2022) 82–100.
[187] B. Jansen, L.P. Goodman, D. Ruiten, Bacterial adherence to hydrophilic polymer–coated polyurethane stents, Gastrointest. Endosc. 39 (5) (1993) 670–673.
[188] G. Costamagna, M. Mutignani, G. Rotondano, et al., Hydrophilic hydromer-coated polyurethane stents versus uncoated stents in malignant biliary obstruction: a randomized trial, Gastrointest. Endosc. 51 (1) (2000) 8–11.
[189] A.M. van Berkel, M.J. Bruno, J.J. Bergman, et al., A prospective randomized study of hydrophilic polymer-coated polyurethane versus polyethylene stents in distal malignant biliary obstruction, Endoscopy 35 (6) (2003) 478–482.
[190] D. Schilling, G. Rink, J.C. Arnold, et al., Prospective, randomized, single-center trial comparing 3 different 10F plastic stents in malignant mid and distal bile duct strictures, Gastrointest. Endosc. 58 (1) (2003) 54–58.
[191] C.I. Kwon, G. Kim, S. Jeong, et al., Bile flow phantom model and animal bile duct dilation model for evaluating biliary plastic stents with advanced hydrophilic coating, Gut Liver 10 (4) (2016) 632–641.
[192] Y. Cheng, B. Wang, Y. Wang, et al., Soluble hydrophobin mutants produced in Escherichia coli can self-assemble at various interfaces, J. Colloid Interface Sci. 573 (2020) 384–395.
[193] C. Andreu, J. Gómez-Peinado, L. Winandy, et al., Surface display of HFBI and DewA hydrophobins on Saccharomyces cerevisiae modifies tolerance to several adverse conditions and biocatalytic performance, Appl. Microbiol. Biotechnol. 105 (4) (2021) 1505–1518.
[194] U. Weickert, F. Wiesend, T. Subkowski, et al., Optimizing biliary stent patency by coating with hydrophobin alone or hydrophobin and antibiotics or heparin: an in vitro proof of principle study, Adv. Med. Sci. 56 (2) (2011) 138–144.
[195] U. Weickert, S. Weddeling, T. Subkowski, et al., Improving biliary stent patency by the use of stent coating - a prospective randomized porcine study, Z. Gastroent. 54 (7) (2016) 629–633.
[196] I. Uysal, A. Tezcaner, Z. Evis, Methods to improve antibacterial properties of PEEK: a review, Biomed. Mater. 19 (2) (2024).
[197] U. Seitz, A. Block, A.C. Schaefer, et al., Biliary stent clogging solved by nanotechnology? In vitro study of inorganic-organic sol-gel coatings for teflon stents, Gastroenterology 133 (1) (2007) 65–71.
[198] D. Ashok, S. Cheeseman, Y. Wang, et al., Superhydrophobic surfaces to combat bacterial surface colonization, Adv. Mater. Interfac. 10 (24) (2023) 2300324.
[199] H. Shao, M. Ma, Q. Wang, et al., Advances in the superhydrophilicity-modified titanium surfaces with antibacterial and pro-osteogenesis properties: a review, Front. Bioeng. Biotechnol. 10 (2022) 1000401.
[200] D.I. Gwon, S.S. Lee, E.Y. Kim, Cefotaxime-eluting covered self-expandable stents in a canine biliary model: scanning electron microscopic study of biofilm formation, Acta Radiol. 53 (10) (2012) 1127–1132.
[201] A. Obermeier, S. Würstle, J. Tübel, et al., Novel antimicrobial coatings based on polylactide for plastic biliary stents to prevent post-endoscopic retrograde cholangiography cholangitis, J. Antimicrob. Chemother. 74 (7) (2019) 1911–1920.
[202] E. Guaglianone, R. Cardines, C. Vuotto, et al., Microbial biofilms associated with biliary stent clogging, FEMS Immunol. Med. Microbiol. 59 (3) (2010) 410–420.
[203] I. Ul Haq, K. Krukiewicz, Antimicrobial approaches for medical implants coating to prevent implants associated infections: insights to develop durable antimicrobial implants, Appl. Surf. Sci. Adv. 18 (2023) 100532.
[204] Z. Sun, L. Ma, X. Sun, et al., The overview of antimicrobial peptide-coated implants against oral bacterial infections, Aggregate 4 (3) (2023) e309.
[205] S. Forbes, A.J. McBain, S. Felton-Smith, et al., Comparative surface antimicrobial properties of synthetic biocides and novel human apolipoprotein E derived antimicrobial peptides, Biomaterials 34 (22) (2013) 5453–5464.
[206] T. Rossignol, B. Kelly, C. Dobson, et al., Endocytosis-mediated vacuolar accumulation of the human ApoE apolipoprotein-derived ApoEdpL-W antimicrobial peptide contributes to its antifungal activity in Candida albicans, Antimicrob. Agents Chemother. 55 (10) (2011) 4670–4681.

[207] C.-H. Lin, J.-C. Lin, C.-Y. Chen, et al., Feasibility evaluation of chitosan coatings on polyethylene tubing for biliary stent applications, J. Appl. Polym. Sci. 97 (3) (2005) 893–902.
[208] S. Bratskaya, D. Marinin, F. Simon, et al., Adhesion and viability of two enterococcal strains on covalently grafted chitosan and chitosan/kappa-carrageenan multilayers, Biomacromolecules 8 (9) (2007) 2960–2968.
[209] H. Liu, N. Huang, Y. Leng, et al., Inhibition of bacterial adherence on the surface of biliary stent materials modified with chitosan, J. Wuhan Univ. Technol.-Materials Sci. Ed. 25 (5) (2010) 795–798.
[210] Y. Toyokawa, S. Kobayashi, H. Tsuchiya, et al., A fully covered self-expandable metallic stent coated with poly (2-methoxyethyl acrylate) and its derivative: in vitro evaluation of early-stage biliary sludge formation inhibition, Mater. Sci. Eng., C 120 (2021) 111386.
[211] T. Ishizawa, N. Makino, Y. Kakizaki, et al., Biosafety of a novel covered self-expandable metal stent coated with poly(2-methoxyethyl acrylate) in vivo, PLoS One 16 (9) (2021) e0257828.
[212] T. Zhang, Q. Liu, F. Meng, et al., Recent advances in stimuli-responsive antibacterial coatings: bacteria-killing and releasing mechanism, design strategies, and potential applications, Prog. Org. Coating 186 (2024) 107923.
[213] Y. Jiang, H. Geng, J. Peng, et al., A multifunctional superhydrophobic coating with efficient anti-adhesion and synergistic antibacterial properties, Prog. Org. Coating 186 (2024) 108028.
[214] Y. Tang, H. Sun, Z. Qin, et al., Bioinspired photocatalytic ZnO/Au nanopillar-modified surface for enhanced antibacterial and antiadhesive property, Chem. Eng. J. 398 (2020) 125575.
[215] J. Yang, H. Xu, L. Zhang, et al., Lasting superhydrophobicity and antibacterial activity of Cu nanoparticles immobilized on the surface of dopamine modified cotton fabrics, Surf. Coat. Technol. 309 (2017) 149–154.
[216] T. Ren, M. Yang, K. Wang, et al., CuO nanoparticles-containing highly transparent and superhydrophobic coatings with extremely low bacterial adhesion and excellent bactericidal property, ACS Appl. Mater. Interfaces 10 (30) (2018) 25717–25725.
[217] Y.Q. Zhao, Y. Sun, Y. Zhang, et al., Well-defined gold nanorod/polymer hybrid coating with inherent antifouling and photothermal bactericidal properties for treating an infected hernia, ACS Nano 14 (2) (2020) 2265–2275.
[218] J. Shi, Y. Lv, L. Yu, et al., Interest of a new biodegradable stent coated with paclitaxel on anastomotic wound healing after biliary reconstruction, Eur. J. Gastroenterol. Hepatol. 25 (12) (2013) 1415–1423.
[219] S.I. Jang, S. Fang, J.H. Nahm, et al., Preclinical evaluation of endoscopic placement of a steroid-eluting metal stent in an in vivo porcine benign biliary stricture model, Sci. Rep. 12 (1) (2022) 8864.
[220] J.R. Lee, S.W. Yang, C.I. Kwon, et al., Anti-fibrotic and anti-stricture effects of biodegradable biliary stents braided with dexamethasone-impregnated sheath/core structured monofilaments, Acta Biomater. 178 (2024) 137–146.
[221] Y. Zhang, K. Chen, H. Liu, et al., A study of a biodegradable braided Mg stent for biliary reconstruction, J. Mater. Sci. 55 (36) (2020) 17170–17182.
[222] L. Guo, L. Yu, Q. Zhao, et al., Biodegradable JDBM coating stent has potential to be used in the treatment of benign biliary strictures, Biomed. Mater. 16 (2) (2021) 025010.
[223] Q. Wang, L. Tan, W. Xu, et al., Dynamic behaviors of a Ca–P coated AZ31B magnesium alloy during in vitro and in vivo degradations, Mater. Sci. Eng. B-Solid State Mater. Adv. Technol. 176 (20) (2011) 1718–1726.
[224] J. Li, W. Xu, X. Lin, et al., A Ca-deficientca-deficient hydroxyapatite (CDHA)/MgF2 bi-layer coating with unique nano-scale topography on biodegradable high-purity Mg, Colloid Surf. B-Biointerfaces 190 (2020) 110911.
[225] G. Keerthiga, M. Prasad, D. Vijayshankar, et al., Polymeric coatings for magnesium alloys for biodegradable implant application, A Review, Materials (Basel) 16 (13) (2023).
[226] L. Wei, Z. Gao, Recent research advances on corrosion mechanism and protection, and novel coating materials of magnesium alloys: a review, RSC Adv 13 (12) (2023) 8427–8463.
[227] Z.Q. Zhang, Y.X. Yang, J.A. Li, et al., Advances in coatings on magnesium alloys for cardiovascular stents - a review, Bioact. Mater. 6 (12) (2021) 4729–4757.
[228] W. Li, Y. Su, L. Ma, et al., Sol-gel coating loaded with inhibitor on ZE21B Mg alloy for improving corrosion resistance and endothelialization aiming at potential cardiovascular application, Colloid Surf. B-Biointerfaces 207 (2021) 111993.
[229] Y. Zhao, J. Bai, F. Xue, et al., Smart self-healing coatings on biomedical magnesium alloys: a review, Smart Mater. Struct. 1 (2023) 100022.
[230] H. Zhang, B. Wang, J. Han, et al., A self-healing coating with embedding of polyphenols on magnesium: towards enhanced corrosion protection for biodegradable vascular implants, Chem. Eng. J. 482 (2024) 149020.
[231] H.P. Heistermann, D. Palmes, U. Stratmann, et al., A new technique for reconstruction of the common bile duct by an autologous vein graft and a biodegradable endoluminal stent, J. Invest. Surg. 19 (1) (2006) 57–60.
[232] Y.L. Liang, Y.C. Yu, K. Liu, et al., Repair of bile duct defect with degradable stent and autologous tissue in a porcine model, World J. Gastroenterol. 18 (37) (2012) 5205–5210.
[233] E. Rezvani Ghomi, N. Nourbakhsh, M. Akbari Kenari, et al., Collagen-based biomaterials for biomedical applications, J. Biomed. Mater. Res., Part B 109 (12) (2021) 1986–1999.
[234] E.E. Montalvo-Javé, G.E. Mendoza Barrera, A.I. Valderrama Treviño, et al., Absorbable bioprosthesis for the treatment of bile duct injury in an experimental model, Int. J. Surg. 20 (2015) 163–169.
[235] R. Margiana, A. Markov, A.O. Zekiy, et al., Clinical application of mesenchymal stem cell in regenerative medicine: a narrative review, Stem Cell Res. Ther. 13 (1) (2022) 366.
[236] C. Zong, M. Wang, F. Yang, et al., A novel therapy strategy for bile duct repair using tissue engineering technique: PCL/PLGA bilayered scaffold with hMSCs, J. Tissue Eng. Regen. Med. 11 (4) (2017) 966–976.
[237] Y. Zhang, A. Sharma, D.J. Joo, et al., Autologous adipose tissue-derived mesenchymal stem cells introduced by biliary stents or local immersion in porcine bile duct anastomoses, Liver Transplant. 26 (1) (2020) 100–112.
[238] S.M. Hosseiniasl, P. Felgendreff, M. Tharwat, et al., Biodegradable biliary stents coated with mesenchymal stromal cells in a porcine choledochojejunostomy model, Cytotherapy 25 (5) (2023) 483–489.
[239] J. Yan, X. Liu, J. Liu, et al., A dual-layer cell-laden tubular scaffold for bile duct regeneration, Mater. Des. 212 (2021) 110229.
[240] I. Boeva, P.I. Karagyozov, I. Tishkov, Post-liver transplant biliary complications: current knowledge and therapeutic advances, World J. Hepatol. 13 (1) (2021) 66–79.
[241] X. Jiang, X. Xiong, Y. Lin, et al., A composite scaffold fabricated with an acellular matrix and biodegradable polyurethane for the in vivo regeneration of pig bile duct defects, Acta Biomater. 150 (2022) 238–253.
[242] F. Sampaziotis, A.W. Justin, O.C. Tysoe, et al., Reconstruction of the mouse extrahepatic biliary tree using primary human extrahepatic cholangiocyte organoids, Nat. Med. 23 (8) (2017) 954–963.
[243] L. Fan, C. Xiao, P. Guan, et al., Extracellular matrix-based conductive interpenetrating network hydrogels with enhanced neurovascular regeneration properties for diabetic wounds repair, Adv. Healthcare Mater. 11 (1) (2022) e2101556.
[244] A. Padalhin, R. Ventura, B. Kim, et al., Boosting osteogenic potential and bone regeneration by co-cultured cell derived extracellular matrix incorporated porous electrospun scaffold, J. Biomater. Sci. Polym. Ed. 32 (6) (2021) 779–798.
[245] J.H. Yea, T.S. Bae, B.J. Kim, et al., Regeneration of the rotator cuff tendon-to-bone interface using umbilical cord-derived mesenchymal stem cells and gradient extracellular matrix scaffolds from adipose tissue in a rat model, Acta Biomater. 114 (2020) 104–116.
[246] R. Khalaj, A.G. Tabriz, M.I. Okereke, et al., 3D printing advances in the development of stents, Int. J. Pharmacol. 609 (2021) 121153.
[247] S.-H. Park, B.-K. Kang, J.E. Lee, et al., Design and fabrication of a thin-walled free-form scaffold on the basis of medical image data and a 3D printed template: its potential use in bile duct regeneration, ACS Appl. Mater. Interfaces 9 (14) (2017) 12290–12298.
[248] J.H. Kim, D.H. Ha, E.S. Han, et al., Feasibility and safety of a novel 3D-printed biodegradable biliary stent in an in vivo porcine model: a preliminary study, Sci. Rep. 12 (1) (2022) 15875.
[249] H. Li, Y. Yin, Y. Xiang, et al., A novel 3D printing PCL/GelMA scaffold containing USPIO for MRI-guided bile duct repair, Biomed. Mater. 15 (4) (2020) 045004.
[250] C.J. Boyer, M. Boktor, H. Samant, et al., 3D printing for bio-synthetic biliary stents, Bioengineering 6 (1) (2019).
[251] Y. Xiang, W. Wang, Y. Gao, et al., Production and characterization of an integrated multi-layer 3D printed PLGA/GelMA scaffold aimed for bile duct restoration and detection, Front. Bioeng. Biotechnol. 8 (2020) 971.
[252] A. Swidsinski, P. Schlien, A. Pernthaler, et al., Bacterial biofilm within diseased pancreatic and biliary tracts, Gut 54 (3) (2005) 388–395.
[253] K.A. Hausegger, R. Kleinert, J. Lammer, et al., Malignant biliary obstruction: histologic findings after treatment with self-expandable stents, Radiology 185 (2) (1992) 461–464.
[254] M.M.A. Verstegen, F.J.M. Roos, K. Burka, et al., Human extrahepatic and intrahepatic cholangiocyte organoids show region-specific differentiation potential and model cystic fibrosis-related bile duct disease, Sci. Rep. 10 (1) (2020) 21900.
[255] J. Li, N. Razumilava, G.J. Gores, et al., Biliary repair and carcinogenesis are mediated by IL-33-dependent cholangiocyte proliferation, J. Clin. Invest. 124 (7) (2014) 3241–3251.
[256] Y. Xiao, J. Wang, W. Yan, et al., Dysregulated miR-124 and miR-200 expression contribute to cholangiocyte proliferation in the cholestatic liver by targeting IL-6/STAT3 signalling, J. Hepatol. 62 (4) (2015) 889–896.
[257] L. Tian, Z. Lu, L. Lei, et al., Preparation, characterization and primary evaluation of trilayered biliary stent films for anti-cholangiocarcinoma and anti-biofilm formation, Int. J. Pharmacol. 606 (2021) 120869.
[258] A.I. Rezk, J. Park, J.Y. Moon, et al., A novel design of tri-layer membrane with controlled delivery of paclitaxel and anti-biofilm effect for biliary stent applications, Nanomaterials 11 (2) (2021) 486.
[259] H. Lee, D.-S. Won, S. Park, et al., 3D-printed versatile biliary stents with nanoengineered surface for anti-hyperplasia and antibiofilm formation, Bioact. Mater. 37 (2024) 172–190.
[260] M.-H. Kang, K.-H. Cheon, K.-I. Jo, et al., An asymmetric surface coating strategy for improved corrosion resistance and vascular compatibility of magnesium alloy stents, Mater. Des. 196 (2020) 109182.
[261] T. Ebrahimi-Nozari, R. Imani, M. Haghbin-Nazarpak, et al., Multimodal effects of asymmetric coating of coronary stents by electrospinning and electrophoretic deposition, Int. J. Pharm. 630 (2023) 122437.
[262] C. Zhang, C. Xu, X. Gao, et al., Platinum-based drugs for cancer therapy and anti-tumor strategies, Theranostics 12 (5) (2022) 2115–2132.
[263] Y. Wang, J. Venezuela, M. Dargusch, Biodegradable shape memory alloys: progress and prospects, Biomaterials 279 (2021) 121215.
[264] G.I. Peterson, A.V. Dobrynin, M.L. Becker, Biodegradable shape memory polymers in medicine, Adv. Healthcare Mater. 6 (21) (2017) 1700694.
[265] Y. Ogawa, D. Ando, Y. Sutou, et al., A lightweight shape-memory magnesium alloy, Science 353 (6297) (2016) 368–370.

[266] J. Liu, Y. Lin, D. Bian, et al., In vitro and in vivo studies of Mg-30Sc alloys with different phase structure for potential usage within bone, Acta Biomater. 98 (2019) 50–66.
[267] H. Abitha, V. Kavitha, B. Gomathi, et al., A recent investigation on shape memory alloys and polymers based materials on bio artificial implants-hip and knee joint, Mater. Today: Proc. 33 (2020) 4458–4466.
[268] G.K. Kulkarni, G.S. Gund, Copper-based shape-memory alloy, in: M.R. Maurya, K. K. Sadasivuni, J.-J. Cabibihan, S. Ahmad, S. Kazim (Eds.), Shape Memory Composites Based on Polymers and Metals for 4D Printing: Processes, Applications and Challenges, Springer International Publishing, Cham, 2022, pp. 93–114.
[269] L.M. Gaetke, H.S. Chow-Johnson, C.K. Chow, Copper: toxicological relevance and mechanisms, Arch. Toxicol. 88 (11) (2014) 1929–1938.
[270] A. Rakshit, K. Khatua, V. Shanbhag, et al., Cu2+ selective chelators relieve copper-induced oxidative stress in vivo, Chem. Sci. 9 (41) (2018) 7916–7930.
[271] B. Gao, Q. Yang, X. Zhao, et al., 4D bioprinting for biomedical applications, Trends Biotechnol 34 (9) (2016) 746–756.
[272] Z. Wan, P. Zhang, Y. Liu, et al., Four-dimensional bioprinting: current developments and applications in bone tissue engineering, Acta Biomater. 101 (2020) 26–42.
[273] S. Amukarimi, M. Mozafari, 4D bioprinting of tissues and organs, Bioprinting 23 (2021) e00161.
[274] Z.U. Arif, M.Y. Khalid, A. Zolfagharian, et al., 4D bioprinting of smart polymers for biomedical applications: recent progress, challenges, and future perspectives, React. Funct. Polym. 179 (2022) 105374.
[275] Q. Yang, B. Gao, F. Xu, Recent advances in 4D bioprinting, Biotechnol. J. 15 (1) (2020) 1900086.
[276] E. Yarali, M.J. Mirzaali, A. Ghalayaniesfahani, et al., 4D printing for biomedical applications, Adv. Mater. 36 (31) (2024) e2402301.